

Politecnico di Torino

Corso di Laurea Magistrale
in Ingegneria Energetica e Nucleare

Tesi di Laurea Magistrale

Integration of distributed resources and storage assets
in distribution networks



Relatore
prof. Massimo Santarelli
Corelatore
prof. Francisco Diaz Gonzalez

Candidato
Francesca Rossi

a.a. 2018/2019

Abstract

Rural grids are distribution networks situated in remote areas, linked to the main grid with long overhead Medium Voltage (MV) lines. These grids are usually characterized by aged infrastructures, that suffer for high vulnerability and low resilience in case of fault. For these reasons rural grids are weak distribution networks that ask from more reliability, higher ability to guarantee a continuous supply in case of fault and a better power quality service. The constitution of Rural Microgrids, able to operate both in grid-connected and in islandmode, can provide a solution. The guarantee of a continuous power supply for the consumers of the microgrid is linked to the increase of self-sufficiency that, nowadays, thanks to the develop and to the cost decrease of technologies, can be based on the exploiting of Renewable Energy Sources (RES). RES generation allows to produce electricity avoiding pollutants emissions but is affected by a variable and low foreseeable electricity production. The integration of Electrical Storage Systems (ESSs) moves to the direction of limiting these issues, providing services as avoiding RES generation curtailment and decoupling in time the production and consumption of electricity. The grid can also benefits from the shaving of peak loads and from the leveling of the load profile.

The aim of this work is to evaluate the technical and economic feasibility and the environmental benefits of a Rural Microgrid characterized by an high photovoltaics (PV) power systems penetration and by the integration of a ESS. The study has been conducted both for a grid of residential users, that constitute a jointly acting self-consumers group, and for a grid including also an industrial load, not related with the self-consumers.

The model proposed has been applied on a study case, represented by a rural grid located in Santa María de Corcó (Girona). From the simulations it results that, in the grid configuration that includes only residential users, the installation of PV systems coupled with the integration of a battery storage system brings significant benefits in terms of reduction of the grid Carbon footprint (up to 81%) and of the increase of the grid self-sufficiency (up to 83,3% of hours per year), and consequently of the independence from the external grid. Concerning the economic aspect, the project is not economically convenient as proved by the evaluation of the investment Pay Back Time (PBT). Thus, taking into account also the economical feasibility, the installation of only PV systems results a good tradeoff between the environmental, reliability and economic grid's needs.

For the grid configuration that includes a factory load can be deduced similar conclusions: the installation of PV systems has a positive effect on the grid and it has a short PBT; the integration of a battery does not result a convenient investment and the improvement from the environmental and grid self-sufficiency point of view are limited, too.

Contents

1	Introduction	8
1.1	Rural Microgrids	9
1.2	Electrical storage systems	10
1.2.1	Mechanical energy storage	10
1.2.2	Electrical energy storage	13
1.2.3	Chemical energy storage	13
1.2.4	Electrochemical energy storage	13
1.3	ESS application in electricity networks	16
1.4	Regulatory framework	17
1.4.1	Economic Barriers to ESS deployment	17
1.4.2	Self-consumption regulation	18
1.5	Electricity Market	20
2	Methodology	28
2.1	DigSILENT Simulations	28
2.1.1	Simulations of the base case and of the high PV penetration case	29
2.1.2	Simulation of the high PV penetration with the battery integration case	29
2.2	Sizing of the battery	35
2.3	Economic Analysis	38
2.3.1	Electricity bills	38
2.3.2	Savings	40
2.3.3	Discounted cash flow analysis	40
2.4	Environmental impact	42
3	Study Case	45
3.1	Description of the microgrid	45
3.1.1	Transformers	45
3.1.2	Residential loads and PV systems	48
3.1.3	Factory	49
3.1.4	Battery	49
3.2	Scenarios	54
3.3	Results	55
3.3.1	Transformers	55
3.3.2	Battery	60
3.3.3	Economic feasibility	66
3.3.4	Environmental impact	68
4	Project Summary	71
4.1	Project Planning	71
4.2	Budget Estimation	71

4.3 Environmental Impact	71
5 Conclusions	73

List of Figures

1.1	SAIDI for unplanned interruption by territorial density, excluding exceptional events. Source: [1]	11
1.2	Unplanned SAIDI for rural areas. Source [2]	12
1.3	Electricity storage technologies' features. Source [3]	12
1.4	Schematic of a Lithium ions battery (LiMO ₂). Source: [4]	14
1.5	Schematic of a half-open Lithium-air ion battery. Source: [4]	15
1.6	Schematic of a Vanadium redox-flow battery. Source: [4]	16
1.7	Energy and power features of batteries used for grid storage application. Source: [4]	16
1.8	Timetable of sessions of the electricity market. Source: [5]	21
1.9	Curve of the offers made by producers. Source[6]	22
1.10	Curve of the bids made by consumers. Source [6]	22
1.11	Match between the offers and bids' curves. Source [6]	23
1.12	Daily evolution of the intraday cost of electricity in Spanish electricity market, in a winter (yellow line) and in a summer (blu line) day. Source [7]	24
1.13	Monthly evolution of the intraday cost of electricity in Spanish electricity market, in a winter (yellow line) and in a summer (blu line) month. Source [7]	25
1.14	Comparison between the daily evolution of the intraday cost of electricity and the VPSC tariff for the "Simplified compensation mechanism". Source [7]	26
1.15	Daily evolution of the old VPSC tariff (valid until the 1 st of April 2019. Source [7]	27
2.1	Flow chart of the instructions executed in the simulations of the first and second scenario. Own elaboration.	30
2.2	Flow chart of the instructions executed in the simulation of the third scenario, model 1. Own elaboration.	32
2.3	Curves of OCV as function of SOC (in charge and discharge mode) obtained from the "Low current OCV" test conducted on a single cell.	33
2.4	Flow chart of the instructions executed in the simulation of the third scenario, model 2. Own elaboration.	34
2.5	Schematic of the electric circuit formed by a battery connected to the AC grid in charge mode. Own elaboration.	36
2.6	CO ₂ emissions and CO ₂ emission factor of the Spanish electrical generation park. Source [8]	42
2.7	Life cycle stages of a PV system. Source [9]	43
2.8	Life cycle Greenhouse Gases (GHG) emissions from rooftop mounted PV systems produced and installed in a Southern European country. Source [9]	43
3.1	Aerial picture of the microgrid.	46
3.2	Diagram of the microgrid obtained from DigSILENT.	47

3.3	Comparison of the weakly evolution of the consumption of load 11 during winter (blu line) and summer (black line).	48
3.4	Comparison of the daily evolution (for one week) of the power generated by the PV system installed in load 16 and in load 20, during winter (blue line) and summer (black line).	49
3.5	Comparison of the net daily profile of load 16 during a winter and summer day.	50
3.6	Comparison of the daily active power factory consumption profile during winter(blue dropped line) and summer (black line).	50
3.7	The battery. Source [10]	51
3.8	Comparison between the grid generation and consumption profile in a winter (top) and summer (bottom) day, referred to the grid configuration without the factory.	52
3.9	Comparison between the grid generation and consumption profile in a winter (top) and summer (bottom) day, referred to the grid configuration with the factory.	52
3.10	Duration curves of the grid configuration without the factory.	53
3.11	Battery capacity required as function of the number of hours during which the grid consumption is covered continuously.	53
3.12	Duration curves of the grid configuration with the factory	54
3.13	Comparison of the daily profiles of the net grid consumption in the three scenarios. Grid configuration without the factory in a winter (left) and summer (right) day.	56
3.14	Comparison of the daily profiles of the net grid consumption in the three scenarios. Grid configuration with the factory in a winter (left) and summer (right) day.	56
3.15	Total apparent Power across the transformers in each scenario (a - c) and comparison between the active power across the transformers and across the battery (d). Grid configuration without the factory.	58
3.17	Total apparent Power across the transformers in each scenario (a - c) and comparison between the active power across the transformers and across the battery (d). Grid configuration with the factory.	60
3.19	Evolution of the SOC during each day of the year. Grid configuration without the factory.	62
3.20	Battery voltage as function of the SOC in charge (a) and discharge (b) mode, referred to the case with a battery capacity of 112 kWh. Grid configuration without the factory.	63
3.21	Battery voltage as function of the SOC in charge (a) and discharge (b) mode for different values of current, referred to the case with a battery capacity of 112 kWh. Grid configuration without the factory.	64
3.23	Battery voltage as function of the SOC in charge (a) and discharge (b) mode, referred to the case with a battery capacity of 177 kWh. Grid configuration with the factory.	65
3.24	Battery voltage as function of the SOC in charge (a) and discharge (b) mode for different values of current, referred to the case with a battery capacity of 177 kWh. Grid configuration with the factory.	66
3.16	Comparison of the transformers duration curves in the three scenarios. Configuration of the grid without the factory.	67
3.18	Comparison of the transformers duration curves in the three scenarios. Configuration of the with the factory.	67
3.22	Evolution of the SOC during each day of the year. Grid configuration with the factory.	68

4.1 Gantt diagram of the project planning. 72

List of Tables

2.1	Characteristics of a LiFePO_4 sample cell. Source [11]	36
3.1	Transformers' characteristics	46
3.2	Peak power and yearly producibility of the PV systems installed in load 16, 17, 19 and 20.	49
3.3	Battery features referred to two battery modules, as the ones shown in figure 3.7. Source [10]	51
3.4	Inverter's features. Source [10]	51
3.5	Battery size calculated for the grid configuration without the factory.	54
3.6	Battery size calculated for the grid configuration with the factory.	54
3.7	Yearly bills and savings evaluated for each scenario.	66
3.8	Investment costs and PBT of the second scenario	66
3.9	Investment costs and PBT of the third scenario.	66
3.10	Carbon footprint of the grid. Configuration without the factory.	69
3.11	Carbon footprint of the grid. Configuration with the factory.	69
3.12	Carbon footprint of the battery.	70

Chapter 1

Introduction

In November 2018 the European Commission presented its long-term strategy for a climate-neutral economy by 2050 [12]. This document is coherent with the goals already fixed in the Energy Roadmap to 2050 (2011) [13] that proposes a reduction of 80-90% of emissions with respect to 1990 level and a complete decarbonization of power sector. To follow this important mission, a deep transition of productive, transportation and urban sector is needed. From the energetic point of view, a series of combined actions have been identified in order to satisfy the need of both fully decarbonization and security of supply. A key role is played by the increase of percentage of RES exploitation, aimed to achieve high rate of coverage in gross final energy consumption, and by the increase of electricity penetration in final-use. The implementation of this scenario can be carried out following two different paradigms: one refers to a global scale with centralized production in few large-size plants based on RES and with HV/UHV transmission systems; the other is developed for a local scale with small-size and distributed generators fed with RES and with a MV/LV distribution system. The first approach is based on Large Interconnections and it is thought for globally share power produced from RES and to consume it in areas far from production sites. The second is based on the creation of Microgrids, flexible and autonomous distribution networks able to work in parallel and separately by the main grid. Even if these two models of production and distribution of electricity follow opposite approaches, it's possible that in the future they could coexist with a proper mix.

Currently Large Interconnections like “Global Energy Interconnection” (GEI) and “The Belt and the Road” (B&R) are scenarios objects of study and of discussion between the involved continents. Differently Microgrids are existing distribution networks, adopted in regions that are hard to connect to the main grid and that take advantage from the possibility of operating independently, in order to guarantee higher reliability and security of supply. These regions are rural or island communities, developing countries with lacking of infrastructures or industrial parks. In order to make Microgrids actually sustainable on an environmental side, distributed generation has to involve technologies with no GHG and pollutants emissions, like photovoltaic (PV) systems on roofs and micro wind turbines. These electricity generators depend on intermittent and fluctuating sources that cause a generation profile with the same behaviour. A grid with an high penetration of RES faces critical issues, not only in covering the whole load demand, but also in grid stability and in assuring standard quality of power injected into the grid. For these reasons RES integration, in particular into Microgrids, requires to be coupled with storage systems, which are able to perform many tasks and to bring benefits for grid management: improve reliability of the grid, operating as backup systems and covering peaks of demand, increase power quality, thanks to frequency regulation, and allow to adopt Demand Response strategies.

A brief overview of Electrical Storage Systems (ESSs) technologies and of their tasks within the electrical system is given in section 1.2, after a description of the main features of Rural Microgrids in section 1.1. Then, in Chapter 2, it is presented the methodology proposed for the design of a rural microgrid with high PV power system penetration and a battery storage system integration. Chapter 3 describes the pilot network adopted as study case and shows the results obtained on the technical, economical and environmental point of view.

1.1 Rural Microgrids

Rural grids are distribution networks situated in remote areas with particular characteristics from the point of view of the orography of the territory and of the meteorological conditions. Rural grids are linked to the main grid with long overhead Medium Voltage (MV) lines and distribute electricity to the customers with Low Voltage (LV) lines. In the past also LV lines were overhead bare cables, while currently they have been replaced, for reliability reasons, with three- of four- wires underground cables. Despite having been carried out this kind of substitutions, rural networks are usually made up of aged infrastructures that suffer for high vulnerability and low resilience in case of fault. Nowadays rural grids are weak distribution networks that ask for more reliability, higher ability to guarantee a continuous supply in case of fault and better power quality service.

The costitution of microgrids in rural areas moves in the direction of providing an economical and sustainable solution to this problems. A microgrid, as defined by the Microgrid Exchange Group of the U.S. Department of Energy (DOE), is "a group of interconnected loads and distributed energy resources within clearly defined electrical boundaries that acts as a single controllable entity with respect to the grid. A microgrid can connect and disconnect from the grid to enable it to operate in both grid-connected or islandmode." [14] The possibility of control the island operational mode on the basis of specific needs and objectives is the streingth point of microgrids and makes them part of the developing of smart grids architecture [15].

The main drivers to the constitution and to the operating control strategies of a microgrid are economical, environmental and of reliability [16]. Especially in remote areas, in order to adjust the grid capability when there is a growing load demand, the constitution and expansion of a microgrid can be cost-effective with respect to the expansion of the transmission system. Besides, another economic advantage can be obtained controlling the connection and disconnection to the main grid on the base of the hourly cost of electricity: in order to minimize the electricity expenditures for consumers the microgrid can be fed by the external grids during hours in which the cost of electricity is lower while the electricity generated or stored within the microgrid can be consumed when electricity price is higher.

Microgrids support also the integration of renewable energy sources, used as means for realizing self-sufficiency and increase independence by fossil fuels, especially in areas affected by fuel volatile prices. As consequence of the increasing RES penetration, environmental and socioeconomic benefits are generated. The environmental benefits are usually quantified in terms of CO₂ emissions avoided, or of other pollutants, likes SO_x, NO_x and particulates, in case of fossil-based power plants replacement. Among the socioeconomic benefits have to be considered the one related to the employment that the renewable energy sector is able to generate [17].

The guarantee of reliability has been in several countries the main drive for the deployment of microgrids: regions affected by weak grids, lack of supply (like in developing countries) or by severe weather conditions, able to generate damages on the transmission systems and outages, can improve the reliability and resiliency of their electricity system

thanks to the higher self-sufficiency provided by microgrids [18]. Since the present work is focused on the study of the developing of a sustainable rural microgrid, the reliability and self-sufficiency needs have a key role in the design choices.

From a statistic point of view, the reliability of an electrical system can be expressed thanks to “continuity indices”, that measure the duration and the number of occurrences of electricity supply interruptions. The expressions of these indices is not identically the same in all the countries: different calculation methodologies are adopted on the basis of the ability of monitoring the interruptions time and occurrences, at different levels and for different kind of events. Different indices are used for transmission and distribution systems, and can be calculated at national level, regional level or for an individual customer, aggregating or not planned and unplanned events. For the Spanish system the TIEPI, or “equivalent interruption time related to the installed capacity”, is used. This index quantify the average time during which the supply to a customer is interrupted and is calculated as:

$$TIEPI = \frac{\sum_i S_i \cdot r_i}{S_T} \quad (1.1)$$

i.e. the sum of the rating of all interrupted MV/LV transformers plus the contracted power of all interrupted MV and HV customers (S_i) times the restoration time for each incident (r_i), over the total rating of all MV/LV transformers plus the total contracted power of all MV and HV customers connected to the system (S_T) [1]. Both figure 1.1 and table 1.2 compare the evolution between 1999 and 2013 of the average time of supply interruptions due to unplanned events for different European countries, disaggregating the data for urban, suburban and rural areas. The SAIDI is the “System Average Interruption Duration Index”, the continuity index used in the majority of the European countries: with respect to the TIEPI is evaluated considering the number of customers affected by the supply interruption, instead of the rating installed power. Even if the calculation method is slightly different, they conceptually express the same parameter.

The last available value of TIEPI for Spanish rural areas is the one evaluated for the year 2011, equal to 119,44 min [2]. This parameter will be considered in section 2.2, in which is explained the methodology used to evaluate the size of a storage system able to guarantee an high level of reliability to a rural microgrid.

1.2 Electrical storage systems

Storage systems are devices that allow to decouple energy production and consumption from a temporal point of view. There are different technologies able to store electricity: they use several physical principle and take advantage from the possibility to convert electricity in other forms of energy.

1.2.1 Mechanical energy storage

The most used ESS in the world, in terms of installed capacity, is Pumping Hydro Storage (PHS): it accounts for 99% of total electricity storage capacity, equal to 127 GW [3]. This system has to be coupled with an hydroelectric power plant and exploits the fluctuation of electricity price during the day: during period in which electricity price is lower, i.e. during night, electricity is used to pump water from the valley reservoir to the upstream one and is, in this way, stored in the form of potential mechanical energy; during the day, when selling electricity is more convenient and the demand is higher, electricity is produced thanks to hydraulic turbines.

Another technology able to store electricity in form of mechanical energy is Compressed Air Energy Storage (CAES). This system uses electricity to compress air (that is stored

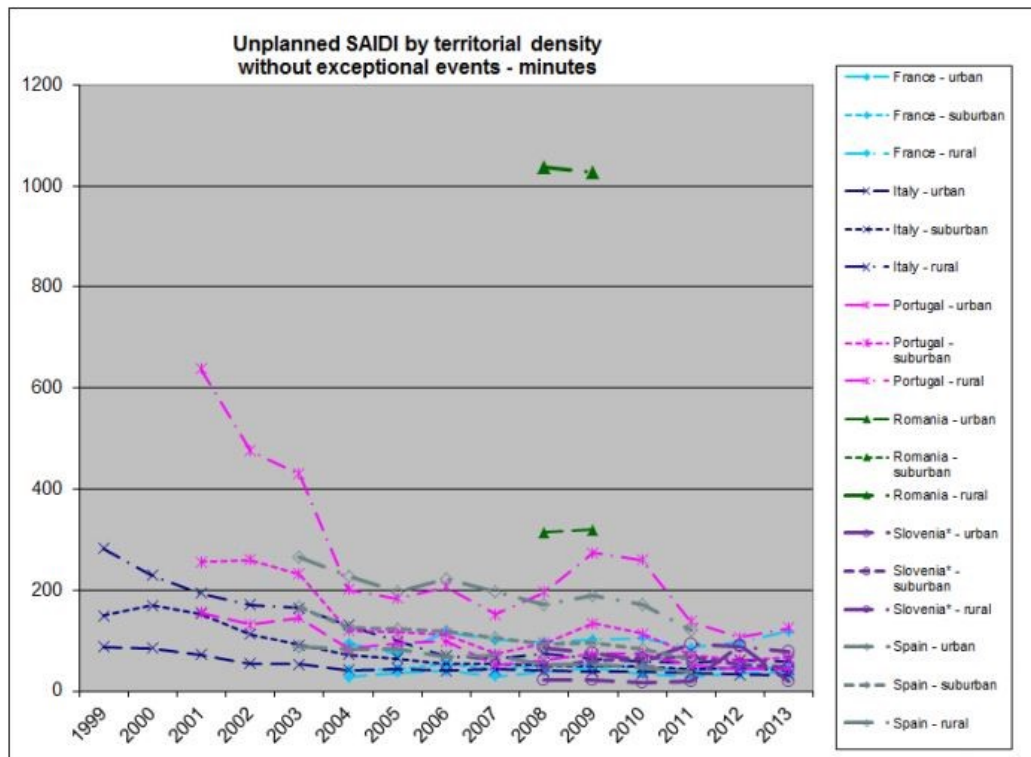


Figure 1.1: SAIDI for unplanned interruption by territorial density, excluding exceptional events. Source: [1]

Country	1999	2000	2001	2002	2003	2004	2005	2006	2007	2008	2009	2010	2011	2012	2013
France						94,2	73,3	116,9	100,4	96,9	102,2	105	86,1	96	118,4
Italy	282,47	229,18	193,7	170,97	165,11	129,82	98,57	69,7	64,84	74,54	64,22	59,42	54,77	59,95	59,01
Portugal			637,53	475,48	429,72	201,64	183,32	206,39	152,38	195,66	273,84	259,74	137,31	105,86	124,86
Romania										1038	1026				
Slovenia*										84,5	74,7	59	92	86,5	78,4
Spain					264,53	228,46	197,7	222,52	196,88	172,24	189,13	171,53	119,44		

Figure 1.2: Unplanned SAIDI for rural areas. Source [2]

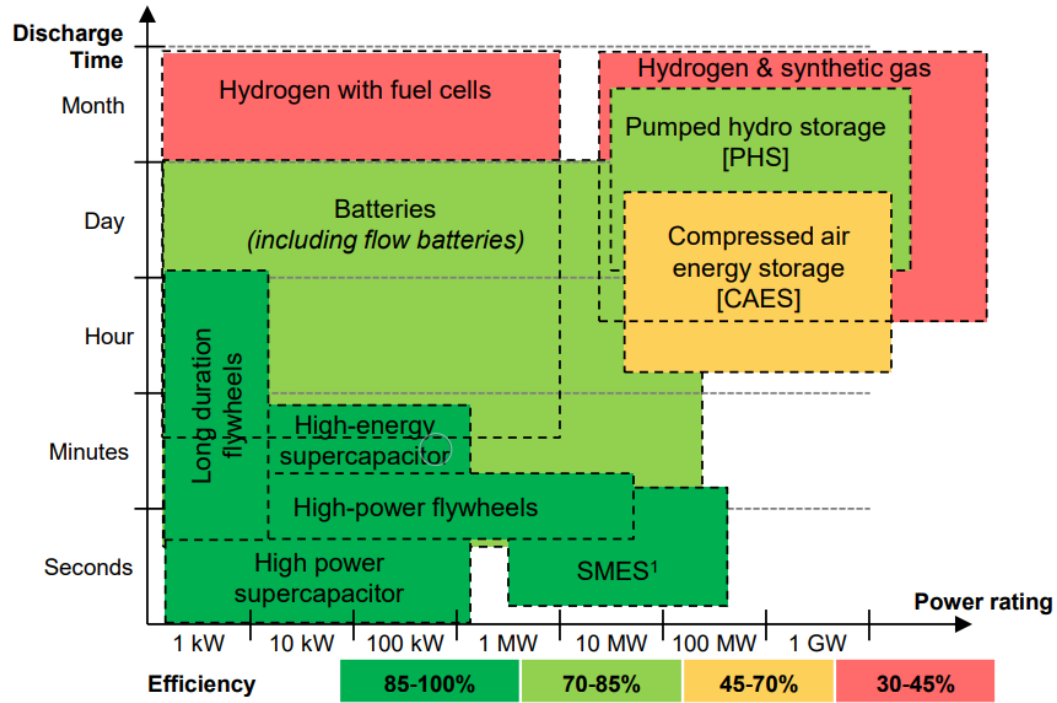


Figure 1.3: Electricity storage technologies' features. Source [3]

underground, into caverns, or under the sea) during the hours of the day in which is more economically convenient or in which there is a surplus in electricity production. The compressed air is then used for feeding a turbogas system.

Both these systems require that the site of installations had particular conditions, like reservoirs separated by a sufficient height difference or the presence of underground caverns. Besides both of them are systems used for bulk power management, which plants are characterized by high rated power and long time of discharge, as shown in figure 1.3.

Among mechanical energy storage there are also Flywheels, systems made up of a shaft connected to an electric generator and of a rotating mass. The mechanical energy is stored in form of potential kinetic energy into the inertia of the rotating part and is released, when required, transmitting the motion to the shaft and to the inductive electric machine. With respect to the technologies previously described, Flywheels are characterized by rated power sensibly lower and by faster discharge time.

1.2.2 Electrical energy storage

Storage technologies based on electrostatic and magnetic phenomena are part of the set of electrical storage. Supercapacitors are condenser with a capacity of thousands of Farad, obtained thanks to the add, between the electrodes, of an electrolyte that forms a double layer of electrostatic charges. Superconductive Magnetic Energy Storages (SMES) are coils of material made superconductive thanks to cryogenic techniques: the coils are immersed in a tank full of liquid Helium or Nitrogen (at around -270°C) and their electrical resistance became null. The electricity injected into the coils is stored within the toroidal magnetic field, generated by the coil itself.

1.2.3 Chemical energy storage

Chemical storage is a typology of electrical storage that can be considered part of the techniques involved in Power-to-X conversion. Power-to-X is a wide concept related to the transformation of surplus of electricity or electricity produced by RES into other products (chemicals with no energy value), services (power-to-heat, power-to-vehicles, power-to-power) or energy vectors (synthetic fuels and hydrogen). The latter results a way to store electricity through an electrochemical and/or a chemical process into the final product:

- Hydrogen can be produced thanks to electrolysis process, feeding an electrolytic cell with electricity;
- Synthetic Natural Gas (SNG) can be produced thanks to simple electrolysis or co-electrolysis followed by methanation reactions;
- other liquid fuels (hydrocarbon compounds) can be obtained starting from syngas and through electrolytic cells.

Among these products, some, like SNG, can be injected in the existing distribution grids while all can be used for power production aims.

1.2.4 Electrochemical energy storage

Electrochemical energy storages are commonly named batteries. The general operating principle of a battery is based on redox reactions that involve materials present in electrodes. Most batteries are in fact closed systems in which during the discharge phase at the anode occur oxidation reaction with the consequent production of ions and electrons. Ions are transported through the electrolyte layer toward the cathode, where reduction occur. Electrons follow the external circuit that connect the electrodes and feed the loads. The process is driven by the gradient of concentration between electrodes. The charge phase is driven by the electrochemical potential provided by the injection of electricity through the external circuit. In this way, at electrodes occur the opposite reactions with respect to the discharge process and the system is restored. Among these kinds of batteries there are Lead acid batteries, Sodium-Sulfur (NaS) batteries and Lithium-ions (Li-ions) batteries.

The most commonly, both for automotive and grid application, are the Li-ions batteries. The combined interest for this kind of batteries in these field has ensured the achievement of a good level of maturity and allows to foresee a decrease of the cost per kWh coupled with an increase of energy density. The latter presents yet good levels if compared with other technologies. These battery, in fact, are characterized by an high energy density, due to the low Lithium ions molecular weight, and high power rate, thanks to the small ionic radius that increases ionic diffusivity. The several Li-ions batteries differ by the cathode materials: while the anode is always in graphite, different cathode structures have been

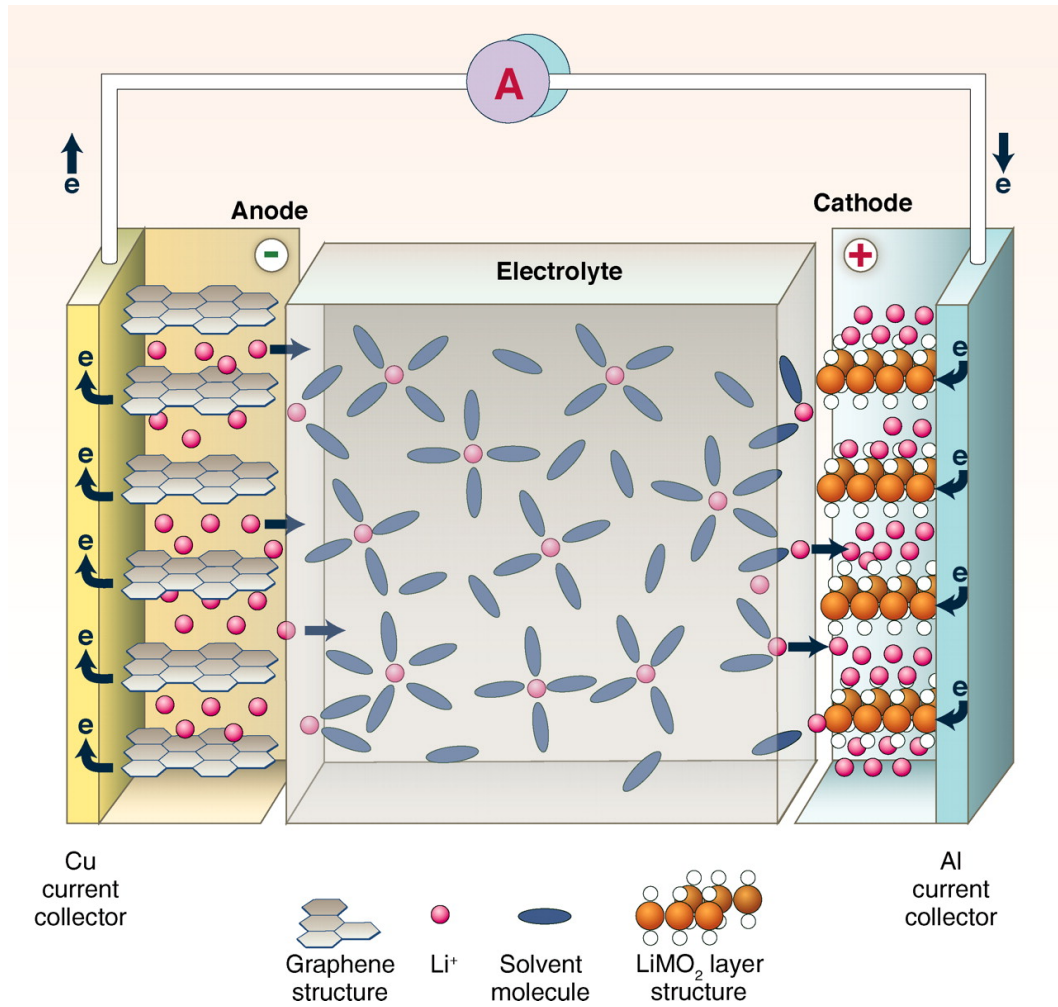


Figure 1.4: Schematic of a Lithium ions battery (LiMO_2). Source: [4]

developed and are still under investigation. The most used are LiCoO_2 cathodes, that belongs to the family of lithiated transition metal oxide cathodes (LiMO_2), and the Lithium Iron Phosphate cathodes (LiFePO_4).

The operating mechanism for both batteries is the one schematized in figure 1.4, that represents a LiMO_2 battery but is valid also for a LiFePO_4 battery. The figure shows the charge process: at the end of the discharge phase the Lithium ions occupy the interspace in the anode structure and, providing electric power from the external circuit, during the charge phase Lithium ions move, crossing the electrolyte, from anode to cathode, restoring the initial condition.

In the case of LiCoO_2 battery the cathode and anode reactions result respectively



and



in which the charge process happens when equilibrium reactions are toward left [19].

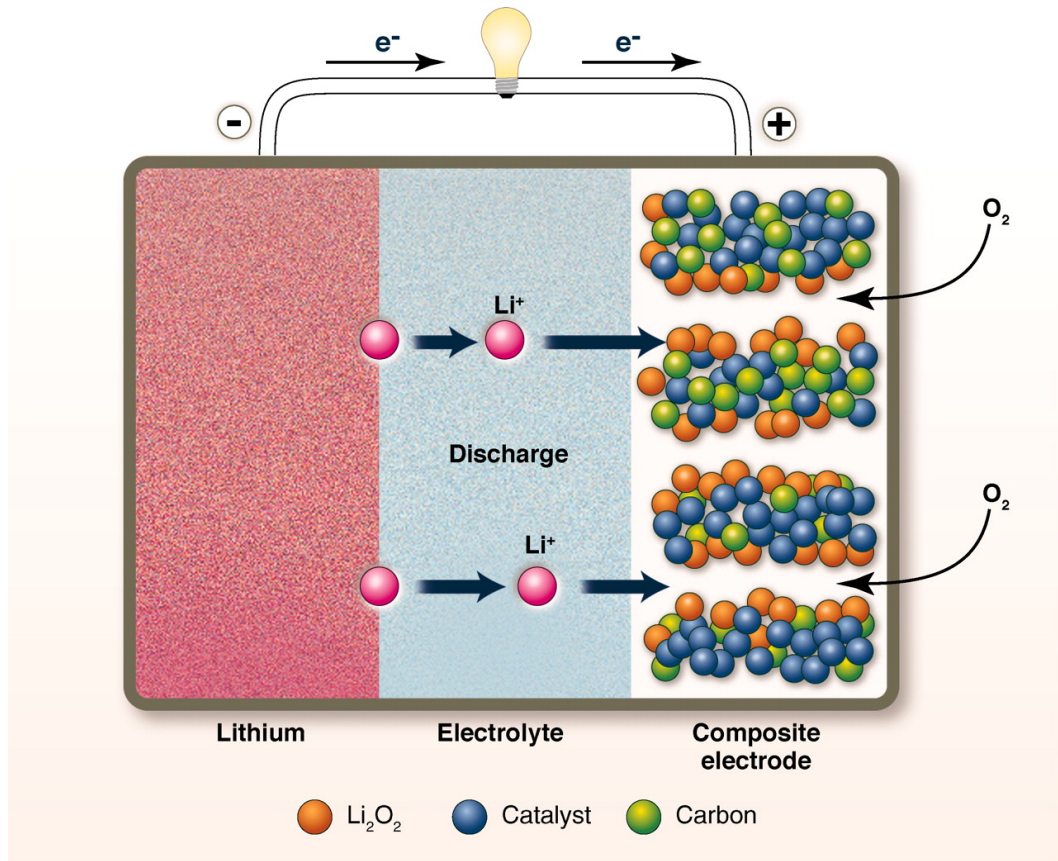
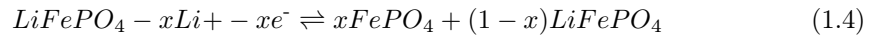


Figure 1.5: Schematic of a half-open Lithium-air ion battery. Source: [4]

In LiFePO_4 batteries the cathode reaction [20] performed is



with equilibrium toward right during charge process. The oxidation anode reaction involves Lithium ions and graphite as shown in reaction 1.3.

For grid application, a long life cycle and an high safety level result very important elements in the choice of the battery. The LiFePO_4 batteries result able to provide higher ciclability (figure 1.7) and higher safety levels with respect to LiCoO_2 batteries [4].

Besides close batteries, half-open and flow batteries exist. Half-open batteries like Li/air (fig. 1.5) and Zn/air batteries, are characterized by one electrode made only of the material that undergoes oxidation (Li or Zn) and the other, usually made of graphite, crossed by air, that perform the reduction reaction.

Flow batteries are able to produce electricity through a chemical looping. The electrolyte of the battery is liquid and is made of two different solutions, continuously recirculated from external tanks. An example of this technology, that is currently knowing a great interest, is Vanadium-Redox battery (fig. 1.6), that exploit the several oxidation states of Vanadium.

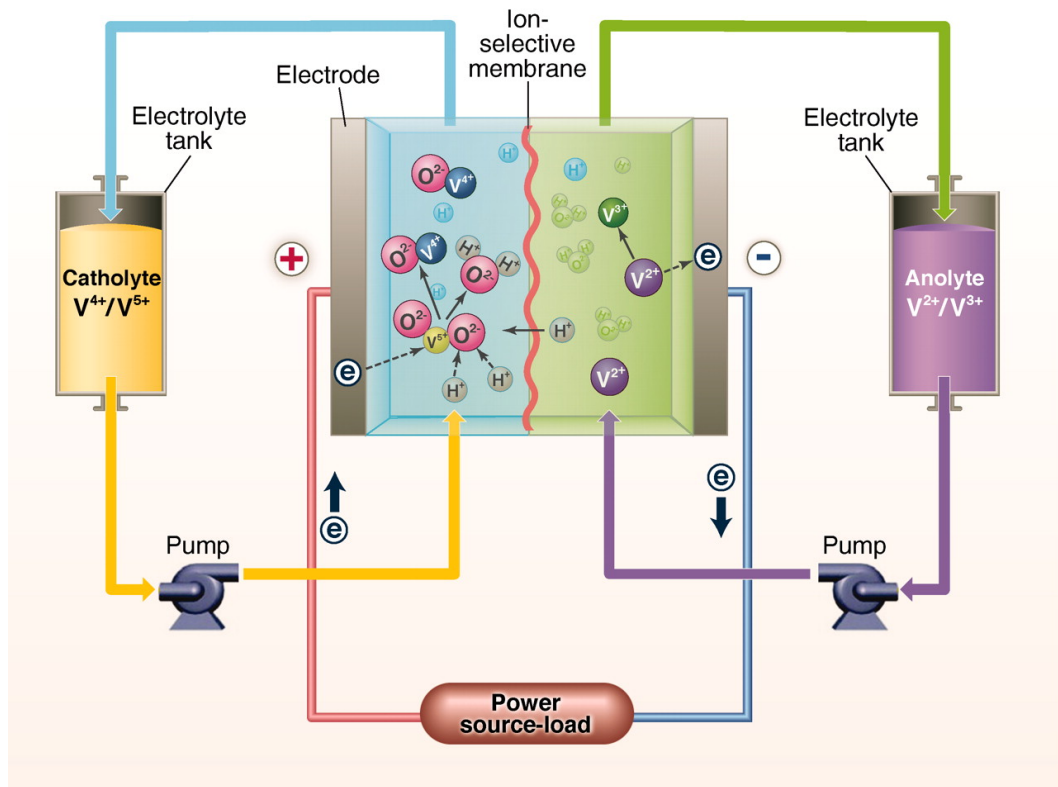


Figure 1.6: Schematic of a Vanadium redox-flow battery. Source: [4]

Battery Type	Voltage Range (V)	Energy Density (Wh/L)	Specific Energy (Wh/kg)	Specific Power (W/kg)	Cycleability
Lead Acid ⁵²	2.1 - 1.8	60 - 75	30 - 40	60 - 110	100 - 500
Nickel-Cadmium ^{53,54}	1.3 - 0.8	130 - 150	40 - 60	40 - 100	2000
Nickel-Metal Hydride ^{55,56}	1.3 - 0.9	250 - 330	70 - 100	70 - 200	1000
Lithium Ion - Li(TM)O ₂ -C TM = Ni, Co, Mn ^{52,58}	4.2 - 2.5	200 - 250	120 - 160	200 - 300	300 - 1000
Lithium Ion - LiFePO ₄ -C ⁵⁷	3.5 - 2.5	120 - 150	80 - 90	200 - 300	1500 - 2000
Lithium Metal-Polymer ^{58,59}	4.0 - 2.4	100 - 110	100 - 110	130 - 170	600
Sodium-Sulfur ⁶⁰	2.1 - 1.8	70 - 150	60 - 120	15 - 70	4000
Sodium-Metal Chloride ⁶¹	2.6	20 - 140	50 - 100	30 - 150	3000
Vanadium Redox Flow ⁶²	1.6 - 1.1	10 - 20	10 - 20	1 - 4	5000

Figure 1.7: Energy and power features of batteries used for grid storage application. Source: [4]

1.3 ESS application in electricity networks

Because of its nature, electric power system has always needed flexibility in order to be able to guarantee a constant demand-supply match and avoid outage and grid's damage.

Flexibility needs can be classified in requirement of stability, balancing and adequacy. The first refers to the control, over a timescale of seconds, of voltage and frequency of the grid. The second refers to the match with loads: the adjustment withrt to the foreseen load profile has to take a time period between minutes and days. The third operates over a long-term period, between months and years, and refers to the need to adjust the generation in order to cover peak demand [3]. The current dominant paradigm used to obtain flexibility is “generation follows the load”. The increase of penetration of renewables resources, and so of variable generation, increases the flexibility needs that can be satisfied adding, within the system, elements with a flexible behaviour, like storage. An high amount of storage capacity could bring to an inversion of paradigm in which “load follows generation” and power system becomes a “time-adjustable” commodity. Below are presented the ways in which a storage can work within a grid, answering to stability, balancing and adequacy needs.

Uninterrupted power supply (UPS): a service that improves the power quality, able to buffer frequency disturbances and provide energy in emergency situations, like black-out.

Black-start capability: ability to restore the right frequency and voltage level and to restart the grid operation after an outage.

Primary control reserve: it consist in frequency regulation, i.e. it limits frequency deviations generated by sudden changes of consumption or failure of generators. This service has to have a fast time of intervention, within thirty seconds from the start of frequency deviation. Besides it results in one of the most promising operational mode from economic point of view because energy requirement are quite low, while market price are relatively high. Considering US Frequency Regulation market, the average capacity need is about 410 MW and the price is in the range of 5-65\$/MWh [21].

Secondary and tertiary control reserve: These services operate in case of imbalance of the grid. The first is automatically activated in few seconds while the other is used as support of the secondary control and is manually activated by the Transmission System Operator (TSO) within fifteen minutes.

Peak-shaving, peak-shifting: through storage is possible to realize load leveling, i.e. cover load peaks with the energy stored instead of withdraw it from the grid. In this way is possible to not increase generation and grid capacity in order to satisfy increasing peaks and to shift production in hours in which is more convenient.

Grid support (GRID) on local scale, at low-voltage grid level, allow to avoid the overload of transformers and to control the power quality thanks to the injection of the necessary active or reactive power.

Residential storage (SELF) allows to increase self-consumption: coupling storage with residential RES generator, like PV on roof, is possible to avoid curtailment during the hours of high RES availability and reducing the amount of electricity withdrawn from the grid. This has a positive effect mostly from the economic point of view.

Island grids can be served by ESS, creating a self-controlled grid and avoiding large infrastructures needed for the connection with the mainland grid.

1.4 Regulatory framework

1.4.1 Economic Barriers to ESS deployment

The achievement of the strategy toward a complete carbon-free energy sector has to consider also the need to modify the rules and the restrictions that define the mode of operation of the energy market. As previously told, the possibility of reaching an high renewable generation penetration is strictly linked to the issue of the integration of energy storage systems. In order to make storage systems know a real diffusion at each level of the electric system, a significant change of the regulatory system is needed aimed at eliminate those factors that,

until today, have hindered their deployment.

The first barrier to the electricity storage system deployment is due to a lack in regulatory framework. In any country's regulation exist a definition exclusively dedicated to energy storage. For this reason there is not a unique and common way to consider storage systems that could be regarded as generators, loads or as an integrated resource of the transmission or distribution system. The most common practice is to consider storage system as generators, even if they are not able to generate a net positive energy flow and without understanding the peculiarity of being able to decouple in time the energy import and export. Besides, this kind of classification has produced a further barrier in the deployment of energy storage in transmission and distribution systems: the EU Directive 2009/72/EC[22] establish that Distribution System Operators can own only small generators (under 50 MW) while Transmission System Operators are not allowed to own and manage any kind of generation systems. On the other side, a change in the regulation, should be oriented forward a definition of storage systems that allow to consider them as integrated in the distribution/transmission networks thanks to their ability to participate in increasing the network's capacity, avoiding other kind of investments, and to provide simultaneously other services economically profitable.

At the same time, the current electricity market regulation, in defining how allocate revenues for the different services required, has played an important role in limiting the affordability of energy storage systems. For example, the participation of storage system in the capacity market is discouraged by the application of penalty in the case in which the system is not able to provide electricity for the whole required period, that is not known or negotiated a priori, increasing the inequity in the competition with traditional power plants. Besides, in order to guarantee a discharging time sufficiently long, the storage system would be forced to maintain a full charge state for long periods, not considering the technical issue concerning this operating condition [23].

Another case is the one related to the providing of ancillary services. The increase of the use of storage systems for Frequency Response services can bring positive effect about emissions reduction and economic savings: would be possible to avoid in one case to utilize power plants operating in partial load condition, in the other to curtail renewables production, realizing at the same time frequency response and balancing service. However, the absence of an ancillary services market able to give value to ultra-fast frequency regulation and balancing doesn't sustain the deployment of energy storage systems in this sector [24].

Whereas these issues remains still open and unsolved, some progresses have been made in the field of residential self-consumption, at regulatory level.

1.4.2 Self-consumption regulation

Within the set of energy proposals included in the "Clean energy for all Europeans" package, which has been completed in May 2019 [25], a good relevance is given to the future role of consumers, both in the electricity production sector and in the electricity market. In the European Directive 2018/2001 of the European parliament and of the council of 11 December 2018 "On the promotion of the use of energy from renewable sources" [26] is written, at article number 76, that: «The Energy Union strategy also recognised the role of the citizen in the energy transition, where citizens take ownership of the energy transition, benefit from new technologies to reduce their bills, and participate actively in the market.»

Besides it's declared that «It is appropriate to allow for the development of decentralised renewable energy technologies and storage under non-discriminatory conditions and without hampering the financing of infrastructure investments.» (Art. 65) The will of creating «non-discriminatory conditions» underlines the need to remove those economical burdens that have been revealed excessive, generating also an unfair competitions with utilities companies.

So in Art. 66 is written : «[. . .]there is a need for a definition of ‘renewables self-consumers’ and of ‘jointly acting renewables self-consumers’. It is also necessary to establish a regulatory framework which would empower renewables self-consumers to generate, consume, store, and sell electricity without facing disproportionate burdens. [. . .]»

In this direction go some of the measures recently issued by the national Spanish government. The first is the elimination of the “Solar Tax”, as established in the Royal Decree 15/2018, also for the injection of electricity in the Low Voltage distribution system. This tax was particularly unfair because was applied to PV generators in order to have access to the grid, both in the case in which the electricity was consumed in the same place or distributed, in a situation in which the law didn’t allow the sale of the surplus of electricity produced and in addition to the taxes paid for distribution. Besides, the evaluation of the “Solar Tax” was based on a fixed amount, related to the size of the PV generator (in terms of rated installed power), and on a variable amount, related to the energy produced. As said, this tax has been canceled also for those PV owners that inject electricity in the distribution system in order to supply consumers located in a different site, giving support to a form of self-consumption different from the individual one. This is the case of “collective self-consumption” or “jointly acting self-consumers” which composition and working principle are better defined in the Royal Decree 244/2019, published on the 5th of April, “in which are ruled the administrative, technical and economic conditions of electric energy self-consumption” [27]. The law defines as collective self-consumption the condition in which a group of consumers are fed by the electricity produced by generators installed “in proximity” to the consumption site. The concept of “proximity” allow to include within the collective self-consumption grid not only the generation plants that are installed in the same place in which the electricity is consumed (defined as proximity plants internal to the consumer’s grid) but also the ones connected in each other point of the grid that develops from the same substation, or that are located within 500 metres from the consumer to which are associated or if consumers and generators are registered in the same cadastral reference. In these cases the generation plant is defined as a proximity plant through the grid.

According to the Law, also storage systems can participate to collective self-consumption if are installed in a site that allow to the system to share its counter-meter with the associated consumer or with the substation that connects the grid with the transmission system.

The law establishes also the different modalities of self-consumption that a single prosumer or a jointly acting set of prosumers can decide to adopt. A first distinction is between the self-consumption supply with or without surplus. The first allows to realize both self-consumption and to inject the electricity surplus in the distribution and transmission networks. As consequence, in this modality it’s possible to individuate two kind of subjects, the consumers and the producers. Besides, if the installed generators are proximity plants through the grid, the producers has to adopt this modality. Who adopt this modality can chose between the possibility of receiving a payment for the electricity injected into the network or not. In order to belong to the first group is necessary to respect some requisites, including that the production units have to be based on renewable primary resources and that their total installed power has to be lower than 100 kW. If one within the listed requirements is not respected, the modality without payment has to be applied. About the modality that doesn’t foresee the injection of energy surplus into the grid, the generators have to be provided with devices able to avoid electricity injection and the only actor identified is the consumer.

For the microgrid that is object of this study, the model of jointly acting self-consumption with the injection in the transmission network and payment of the surplus electricity has been adopted. In particular, the methodology used to evaluate the yearly bills and savings for the prosumers follow what is prescribed in the same Royal Decree 244/2019 and is indicated as “Simplified compensation mechanism”. This mechanism allows to adopt the

following tariffs:

- the voluntary price for small consumers (VPSC) or “precio voluntario para el pequeño consumidor” (PVPC) in Spanish, for the purchase of electricity;
- the hourly intraday cost for the sale of the electricity surplus.

A more detailed description of these kind of tariffs is given in section 1.5.

In any case the economic value of the hourly energy surplus can be higher than the one of the hourly energy consumed during the invoicing period, that can last maximum a month.

In the final part of the Law is further clarified the methodology to follow in order to calculate and allocate the amounts of energy produced, self-consumed and injected into the grid between the prosumers. In the agreement signed between all the participants to the collective self-consumption, for each prosumer are expressed the values of the allocation coefficient of the energy generated (β_i) and the allocation coefficient of the net energy generated (α_k). Both the coefficients have to maintain constant values in the whole invoicing period. If not expressly defined with other formulations, according to all the prosumers enjoying the modality of collective self-consumption, the ones proposed into the law are:

$$\beta_i = \frac{Pc_i}{\sum_i Pc_i} \quad (1.5)$$

and

$$\alpha_k = \frac{PI_k}{\sum_k PI_k} \quad (1.6)$$

where Pc_i and PI_k are the contracted consumption and generation power for each i -th consumer and each k -th generation plant, respectively.

1.5 Electricity Market

Spanish electricity market is regulated by the Royal Decree 2019/1997 and managed by the Iberian Electricity Market (MIBEL), which the Market Operator OMI-Polo Español S.A. (OMIE) refers to. As in the others countries, the electricity market is composed by futures markets, day-ahead market, intraday market and system adjustment services. Each of these markets is based on a different time frame and evaluates the cost of electricity using a mechanism of matching between the bids for sale and for purchase.

The future market is a long term/medium term forward market which establishes the electricity price with an advance of years or months with respect to the moment in which it will be produced and consumed. To this market mainly participate electricity producing companies and the Distribution Companies, but can be joined also by consumers who chose to buy electricity directly from the market. The aim of this market is to determine a fixed electricity price in order to make the interested parties avoid the risk of the uncertainty of the day ahead market. However, the methodology used to evaluate the electricity price in the future market is a kind of foreseen of the day ahead cost because takes into account the same element of influence: on the supply side the factors considered are the forecast of the fuel price, of the renewable production, of the availability and of new entry into operation of generation power plants; on the demand side is necessary to foresee how it will evolve, both in terms of energy and power peaks, and the weather conditions.

The other markets are aimed to determine the hourly price of electricity of the day in which it will be actually produced and consumed. The day ahead, the intraday and the adjustment markets operate on a time frame since one day until few minutes before the

HORARIO DE LAS SESIONES DEL MERCADO DE ELECTRICIDAD							
	MERCADO DIARIO	MERCADO INTRADIARIO					
		1ª SESIÓN	2ª SESIÓN	3ª SESIÓN	4ª SESIÓN	5ª SESIÓN	6ª SESIÓN
Apertura de sesión		16:00	21:00	1:00	4:00	8:00	12:00
Recepción contratos bilaterales	10:00						
Integración de las posiciones abiertas del mercado a plazo	10:00						
Cierre de sesión	10:00	17:45	21:45	1:45	4:45	8:45	12:45
Casación	11:00	18:30	22:30	2:30	5:30	9:30	13:30
Publicación del programa base de funcionamiento (PBF)	12:00						
Recepción de desagregaciones	12:00	Durante 30 minutos posteriores a la publicación de los resultados de la casación					
Análisis de restricciones	14:00	19:10	23:10	3:10	6:10	10:10	14:10
Publicación del programa diario viable (PVD)	16:00						
Publicación del programa horario final (PHF)		19:20	23:20	3:20	6:20	10:20	14:20
Anotaciones en cuenta para seguimiento de garantías	11:00	19:15	23:15	3:15	6:00	9:40	15:30
HORIZONTE DE PROGRAMACION	24 horas	28 horas	24 horas	20 horas	17 horas	13 horas	9 horas
Periodos horarios		21 - 24	1 - 24	5 - 24	8 - 24	12 - 24	16 - 24

Source: OMEL

Figure 1.8: Timetable of sessions of the electricity market. Source: [5]

purchase of the electricity. In particular the adjustment services are the one applied shortly before the electricity dispatchment, generally asking to the generators to make economical bids for deviate their production with respect to the one previously contracted, in order to reply to a supply demand unbalance. Figure 1.8 shows the timetable followed by electricity market every day.

The day ahead market stops receiving bids for the purchase and sale of electricity of the successive day at 10 a.m. and publishes the price at 12 a.m. The mechanism used to evaluate the price at which electricity will be sold is based on the evaluation of the curve of the generators' offers and of the curve of the customers' bids. The generators have to specify how much energy and at which minimum and maximum (that in Spanish market can't exceed 180 euro/MWh) price are they able to provide. The price offered is referred only to the "opportunity" cost, that reflects the amount of money asked by generators to don't shift the production in another moment. For this reason, the power plants than can operate with higher flexibility can make higher offers and are in the higher part of the curve: belong to this group adjustable hydroelectric power plants, which opportunity cost is associated to the possibility to use the water reservoir in another moment. Lower is the possibility to regulate the production, like for nuclear power plants, RES generators and thermoelectric plants that can't participate to the fuel market, lower is the offer that they can make and lower their position in the curve.

The curve of the demand, in figure 1.10, is built with the bids made by the consumers: as for producers they have to specify the amount of energy required and the range of money in which are willing to buy electricity. Market companies are used to bid the maximum, i.e. 180 euro/MWh, in order to be sure to guarantee supply to their consumers. Consumers that can easily shift their consumption, like PHS systems or some factories, can make lower bids and accept to adjust their consumption following market's prices.

The price of electricity will be the same for all generators and consumers, following the regulation of a marginal market: this price is calculated as the intersection between the offer and demand (figure 1.11).

The same methodology, of collecting and matching offers and bids, is used in the intraday market, in order to define the electricity price for each hour of the day: the price resulted by the day ahead market is adjusted following the needs of the participants to the market in real time. This market is organized in six sessions: as indicated in figure 1.8, the first starts at 21 p.m. of the previous day and lasts 28 hours, the last starts at 16 p.m. of the day in question and is related to the last 9 hours. The result of the intraday market is

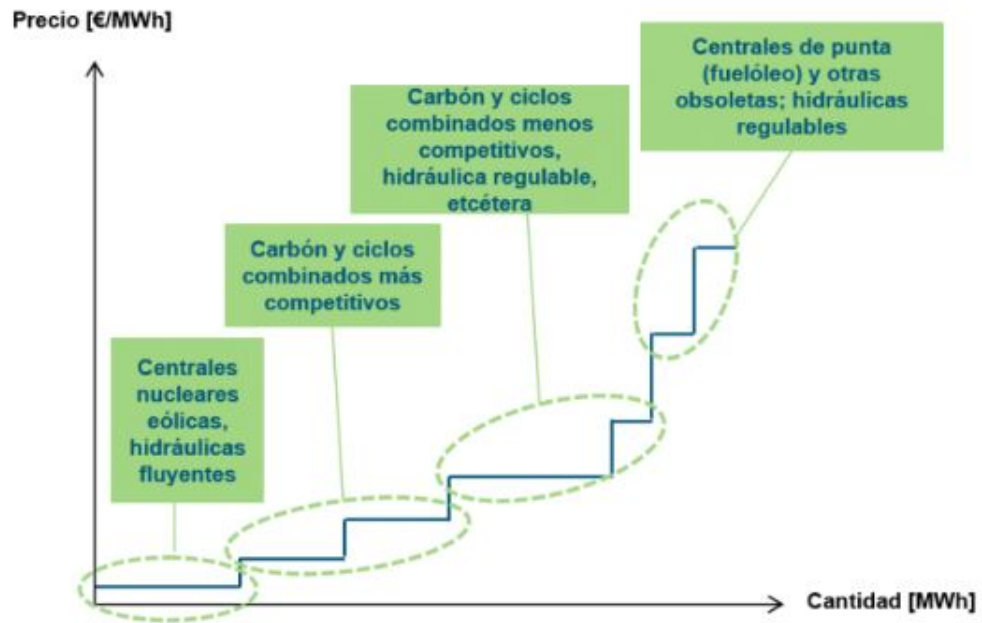


Figure 1.9: Curve of the offers made by producers. Source[6]

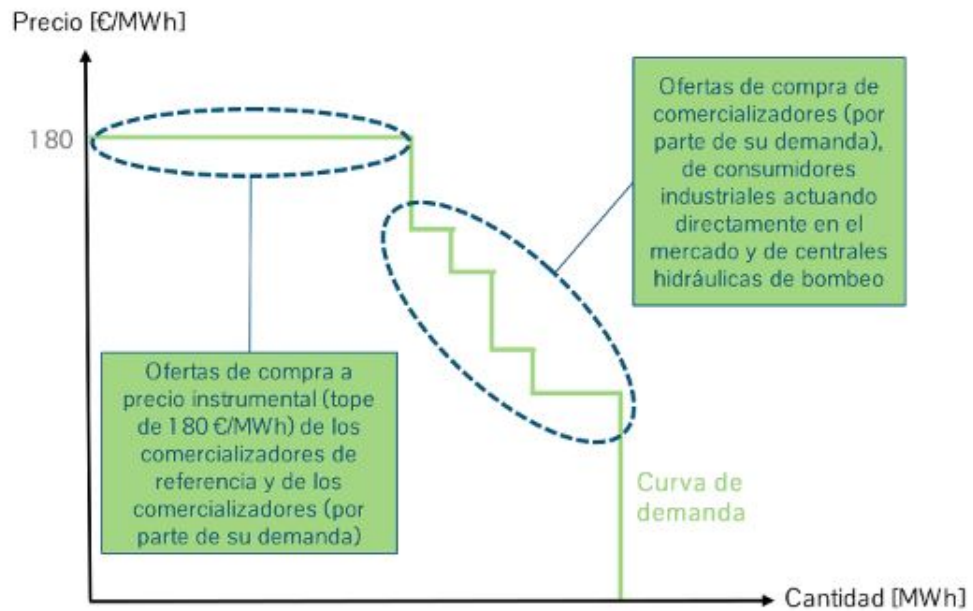


Figure 1.10: Curve of the bids made by consumers. Source [6]



Figure 1.11: Match between the offers and bids' curves. Source [6]

an hourly electricity tariffs that shows, during each day, periods of peaks and of valleys. Figure 1.12 shows the evolution of the hourly intraday cost for a summer (blue line) and winter (yellow line) day. During the winter day the presence of two peaks period, around 9 a.m. and 8 p.m., associated to the periods of higher consumption, is more evident. As consequence there are also two deep valley periods, once during night and the other during the afternoon. Summer tariff results almost always higher than winter one: this is more clear in figure 1.13, where is shown a monthly comparison between January and July.

The hourly intraday tariffs, called “Precio medio horario” in Spanish, is the price at which consumers that realize self-consumption can sell the surplus of electricity generation, following the “Simplified compensation mechanism”. According to this mechanism, the amount of electricity that exceed the self-consumption and has to be supplied by the grid can be bought at VPSC tariff. This tariff is in effect since the 1st of April 2014 and is an hourly tariff dedicated to consumers with a contracted power lower than 10 kW. After the publication of the Royal Decree 244/2019, a new VPSC, specific for the excess in self-consumption with “Simplified compensation mechanism”, has been proposed. This tariff is in effect since the 1st of April 2019 and daily evolution is shown in figure 1.14, in comparison with the intraday cost of electricity.

Because of a lack of availability of data, the tariff adopted in this work for the simulation of the economic part is the old VPSC. This tariff develops on two daily periods how shown in figure 1.15.

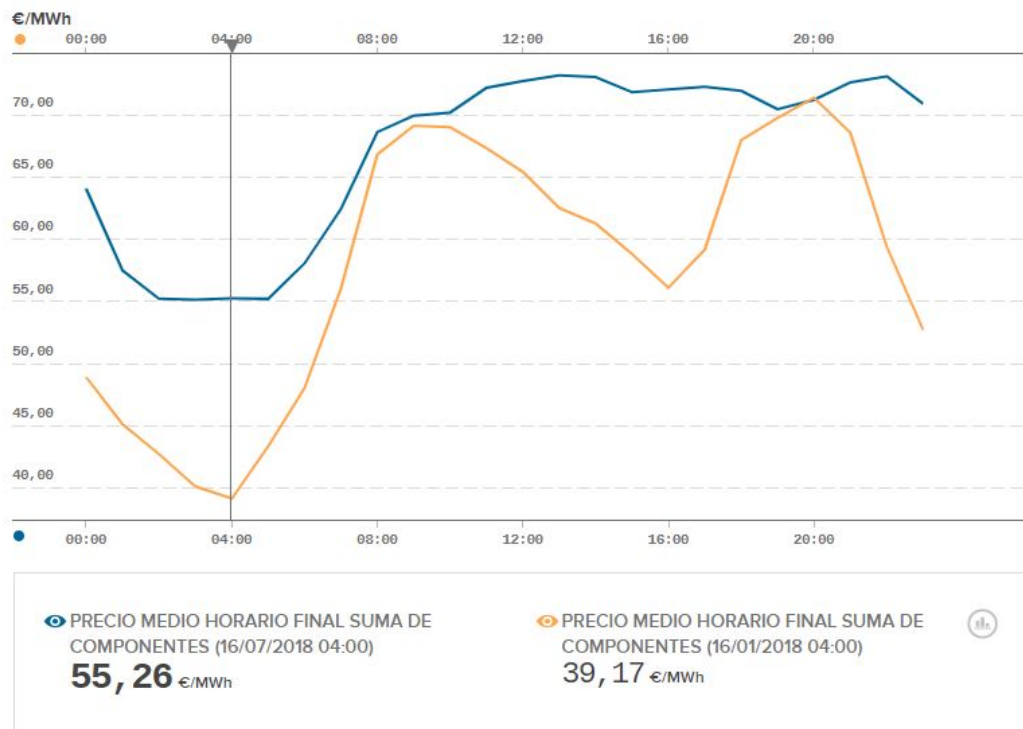


Figure 1.12: Daily evolution of the intraday cost of electricity in Spanish electricity market, in a winter (yellow line) and in a summer (blue line) day. Source [7]

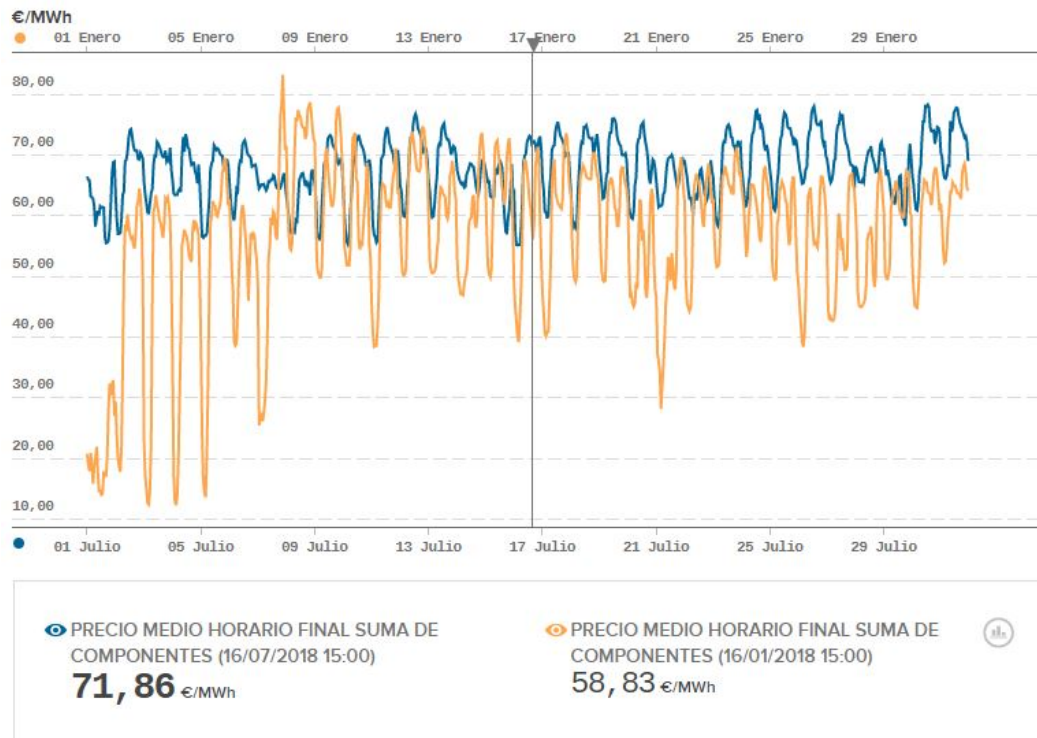


Figure 1.13: Monthly evolution of the intraday cost of electricity in Spanish electricity market, in a winter (yellow line) and in a summer (blue line) month. Source [7]

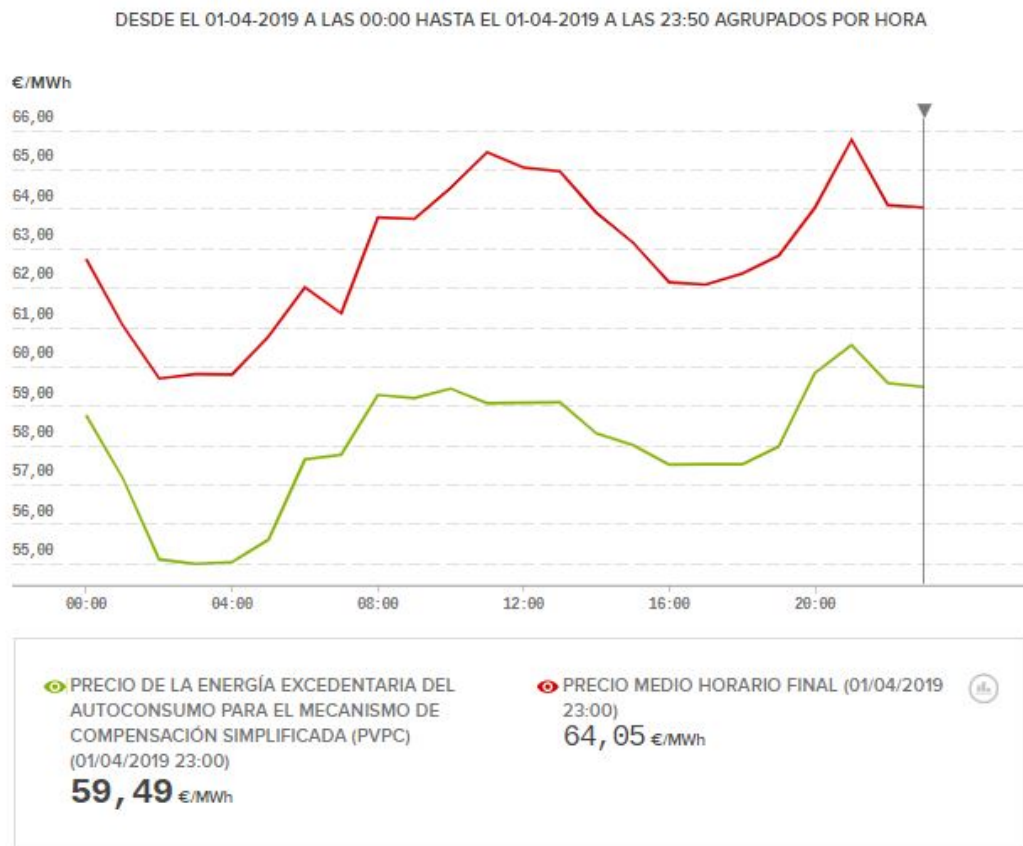


Figure 1.14: Comparison between the daily evolution of the intraday cost of electricity and the VPSC tariff for the "Simplified compensation mechanism". Source [7]



Figure 1.15: Daily evolution of the old VPSC tariff (valid until the 1st of April 2019). Source [7]

Chapter 2

Methodology

In this chapter is described the methodology used to simulate the behaviour, to assess the economical feasibility and to evaluate the environmental impact of a microgrid with an high PV penetration, with and without battery storage system.

Two grid's configurations are object of study and reveal some peculiarities that bring to the elaboration of slightly different solutions. The first configuration is the one of a grid composed only by residential users that, from the regulatory and economic point of view, form a jointly acting self-consumption community. The second one is characterize by the presence of a factory that stands out for an higher consumption profile, both in terms of active and reactive power, and that doesn't participate to the self consumption.

The aim of the simulations conducted is to verify the ability of the grid to bear the installation of an high amount of renewables electricity generation and to evaluate which kind of benefits the integration of a storage system is able to bring. Then, from the analysis of the new net power exchange with the external grid, economical and environmental considerations are carried on.

2.1 DigSILENT Simulations

The software used in order to simulate the microgrid is DigSILENT Power Factory, an appropriate software for the analysis of transmission, distribution, generation and industrial systems. The peculiarities of this software are the possibility of graphically building the grid and its ability in computing load flow calculations.

The scenarios simulated are referred to three different consumption and generation profiles of the loads and PV generators that are within the microgrid. The base case is the one in which there are not PV systems installed and the microgrid is fed only by the transmission network. Then, to the same consumption profiles, PV generation profiles are applied in all the residential loads and a jointly acting self-consumers group is formed. This scenario represents the condition of high PV penetration. Finally a battery is added into the grid, with the aim of storing the PV generation surplus and feeding the grid during the hours of absence of PV generation.

The base case and the scenario with high PV penetration are simulated using the same method and the same scripts. The third case has to take into account the presence of the battery and the instruction for the simulation of its operating modes.

2.1.1 Simulations of the base case and of the high PV penetration case

The scheme of figure 2.1 represents the steps followed, and executed by the relative scripts, in order to simulate the base case and the one of a microgrid with high PV penetration.

The construction of the grid consists in the setting of the elements used for the grid modeling. The external grid is represented by voltage sources, connected to the microgrid with winding transformers. Then for each hour (in the while loop) the network has to be configured, i.e. imposing the voltage at the external grid side and the active and reactive power at each load. A load flow calculation is performed which, solving power flow equations, is able to compute the voltage at each bus and the current flowing in each line. Through the software is possible to determine also the value of active and reactive power across each bus. The most of the interest is for the buses of the transformers: the results exported are the active and reactive power of the transformers that represent the net power balance between the external grid and the microgrid.

2.1.2 Simulation of the high PV penetration with the battery integration case

The battery system, composed by the battery itself and its DC/DC converter and DC/AC inverter, can be modeled as a load. For this reason is necessary to consider that the signs of the values of power and current has to follow the convention of loads: positive in charge mode and negative in discharge. The simulation is composed by three sections. The first is identically the same of the simulation conducted for the second scenario, and is omitted in the schemes of figures 2.2 and 2.4. The obtained results about transformers buses allow to know the needs of the grid and are used to size the battery (second part of the simulation). The methodology used to determine the capacity of the battery is the one described in section 2.2. How will be explained, several values of capacity will be considered: thus, the simulation of the third part is conducted for each battery value. The third section is the one that contains the instructions for the operational mode of the battery. This part of the simulation has been conducted with two models, with a different level of analysis: the first one, represented by the scheme of figure 2.2, takes into account only the power exchanged by the battery and the microgrid; the second one (scheme of figure 2.4) studies more in detail the behaviour of the battery, in terms of voltage between its extremities, and calculates in a more accurate way the state of charge (SOC). The following paragraphs describe how the two models work.

Battery model 1

For each hour of the year is calculated P_h , the sum of the active power measured at the transformer buses $P_{T1,h}$ and $P_{T2,h}$.

A positive value of P_h means that the PV generation is not sufficient to cover the needs of the microgrid and that electricity would be required from external grid. If the amount of energy stored ($E_{\text{stored},h}$) into the battery is not null the grid can be fed by the battery instead of by the external grid. To impose this condition, i.e. the discharge operational mode, the active power of the load representing the battery is set equal to $-P_h$, if the amount of energy stored is higher than the power required, or equal to $-E_{\text{stored},h}$, if the latter is lower than P_h .

The charge operational mode is executed if P_h is negative, that means that there is a surplus of PV generation that would be injected into the external grid. Also in this case the active power of the battery is set equal to $-P_h$, in order to obtain a positive value of power absorbed, if storing this surplus into the battery doesn't overcome its total capacity.

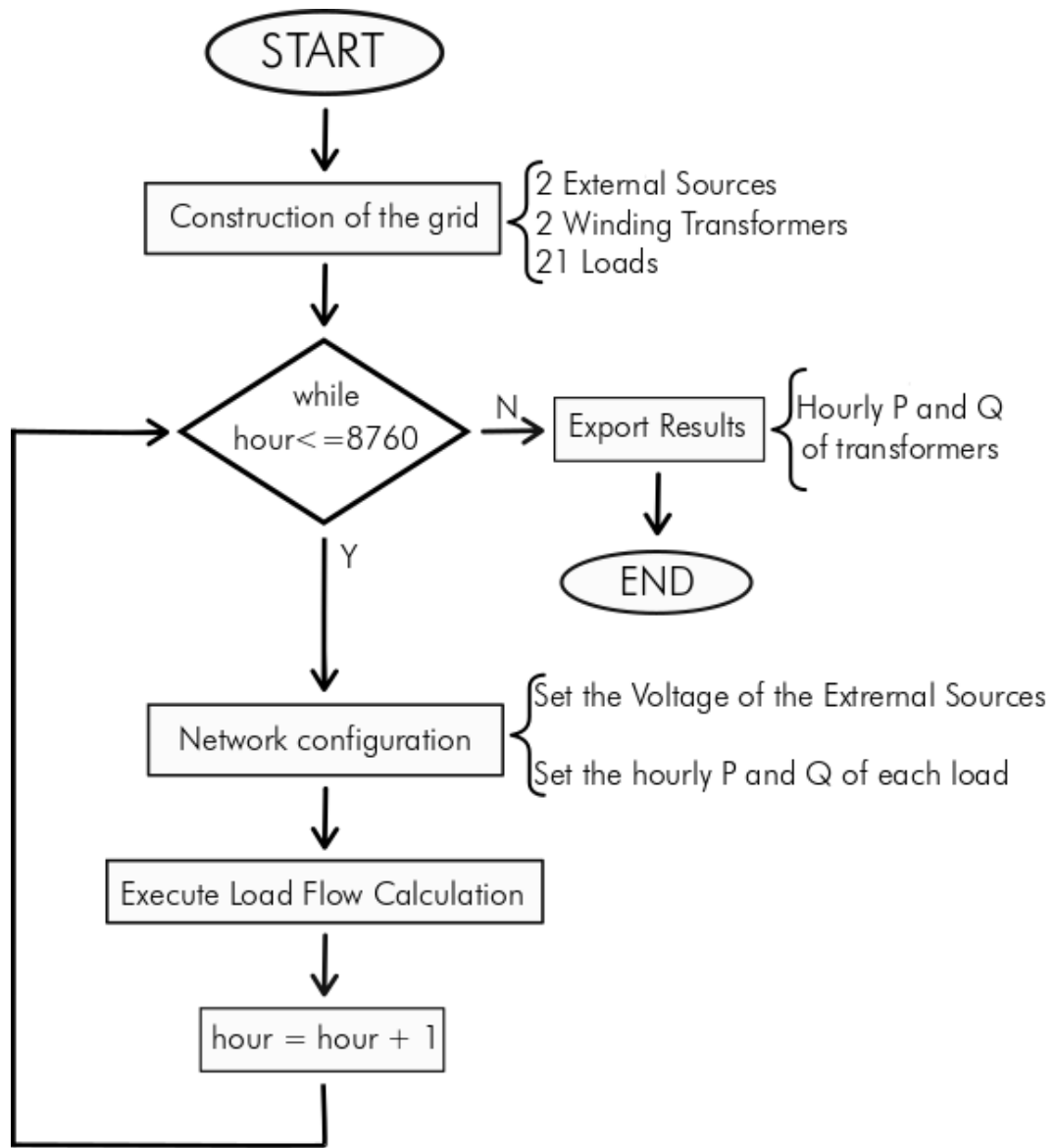


Figure 2.1: Flow chart of the instructions executed in the simulations of the first and second scenario. Own elaboration.

Otherwise the amount of electricity stored into the battery is evaluated as the difference between its total capacity and the $E_{\text{stored},h}$. After having determined and set the operational mode of the battery, the value of energy stored into the battery is updated:

$$En_{\text{stored},h+1} = En_{\text{stored},h} - P_h \cdot \Delta t \quad (2.1)$$

where Δt is equal to 1 hour.

Then the network is configured and a load flow calculation is performed. At the end of the simulation time period, the results exported are the ones related to the power at transformer buses and the power and SOC of the battery.

Battery model 2

In this simulation the instructions related to charging and discharging operational mode of the battery follow the same logical conditions explained in the previous section. The difference is in the methodology used to model the behaviour of the battery. The SOC is evaluated in a more accurate way applying the expression:

$$SOC_{h+1} = SOC_h \pm \eta i \cdot \Delta t \frac{I_h}{Cap} \quad (2.2)$$

where SOC_h and SOC_{h+1} are respectively the state of charge, expressed as a percentage of the total capacity, at the beginning and at the end of a discharge or charge time period Δt , equal to 1 hour. ηi represents the efficiency related to self-discharge phenomena, and is posed equal to 1. I_h and Cap are the current flowing in the battery in the time interval between h and $h+1$ and the capacity of the battery, expressed in Ah, respectively. How to evaluate the capacity of the battery in Ah is explained in section 2.2.

The higher accuracy of this method is due to the capability of modeling the relations between the current, the voltage and the SOC. These parameter are not independent one from the others. The working points of a battery, both in charge and discharge mode, are identified by the polarization curve, in the plane IV. The general equations of a polarization curve of the charge and discharge operational mode are

$$V(I) = OCV + R_c \cdot I \quad (2.3)$$

$$V(I) = OCV - R_d \cdot I \quad (2.4)$$

where the ohmic resistances R_c and R_d model the losses due to mass and charge transport phenomena inside the battery. Besides the SOC reflects a different condition in terms of amount and concentration of reactants and this affect, from an electrochemical point of view, the Gibbs free energy of the reaction and, consequently, the OCV. From Nernst equation

$$OCV = \frac{\Delta g_{\text{react}}}{z \cdot F} \quad (2.5)$$

where g_{react} is the molar Gibbs free energy of the reaction, z the number of electrons involved in the redox reactions and F the Faraday' constant. The lower is the SOC, lower is the concentration of reactants and lower is the electrochemical driving force of the reaction: for this reason also the OCV is lower. Figure 2.3 shows the curves of OCV as function of the SOC referred to a single sample cell.

Thanks to a "Low current OCV" test is possible to assess the evolution of OCV during a discharge and charge cycle and to extrapolate the corresponding SOC. The test is performed applying a pulse current for a period necessary to generate a $\pm 10\%$ of SOC variation and

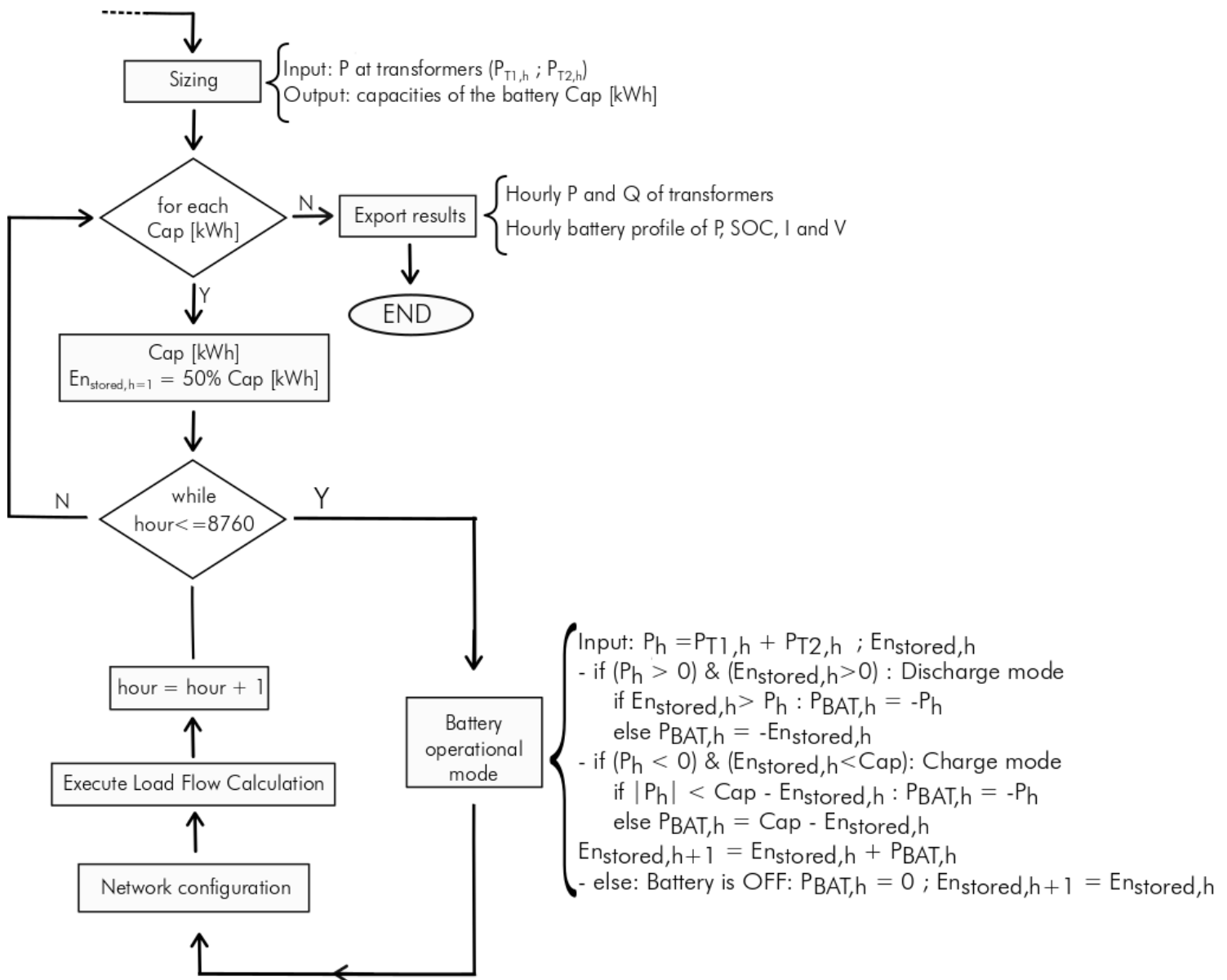


Figure 2.2: Flow chart of the instructions executed in the simulation of the third scenario, model 1. Own elaboration.

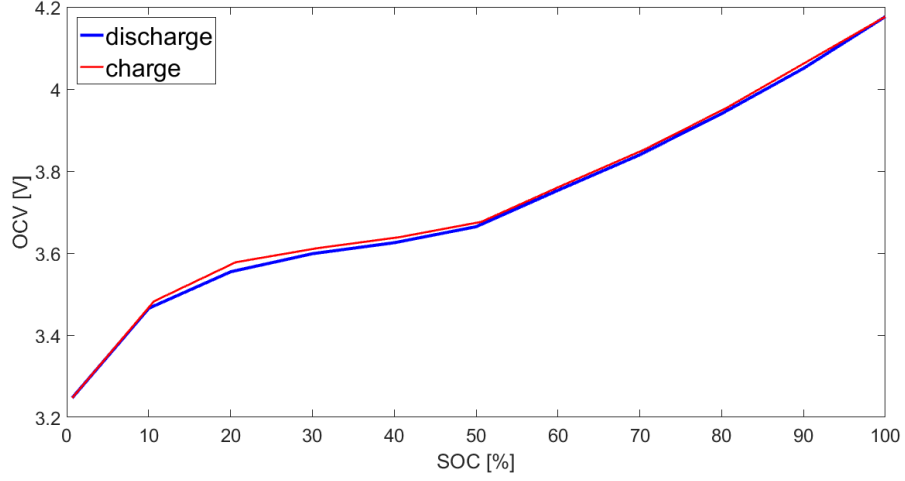


Figure 2.3: Curves of OCV as function of SOC (in charge and discharge mode) obtained from the "Low current OCV" test conducted on a single cell.

measuring, after a restoration period, the value of OCV. The points of the obtained curves are used in the simulation in order to evaluate the OCV of the battery, known its SOC, applying a linear interpolation.

As shown in the scheme of figure 2.4, after having determined the required battery operational mode, the related script is executed: known the value of the internal battery resistance and the SOC_h , the current, the voltage across the battery and SOC_{h+1} (at the end of the charge/discharge period) are calculated. The current flowing through the battery (I_h) is calculated solving the equation

$$|P_h| = V_h \cdot I_h \quad (2.6)$$

where the expression of the voltage measured at the ends of the battery (V_h) is

$$V_h = (OCV_h \pm \frac{R_{c/d} \cdot I_h}{N_p}) N_s \quad (2.7)$$

where OCV_h , that is both the value of the OCV of a single cell and the equivalent voltage of a string of parallel cells, is calculated through a linear interpolation based on the value of SOC_h .

The equation 2.6 became

$$|P_h| = (OCV_h \pm \frac{R_{c/d} \cdot I_h}{N_p}) N_s \cdot I_h \quad (2.8)$$

that solved for I_h is

$$I_{h, c/d} = \frac{\mp OCV_h \cdot N_s \pm \sqrt{(OCV_h \cdot N_s)^2 \pm 4|P_h|R_{c/d} \frac{N_s}{N_p}}}{2R_{c/d} \frac{N_s}{N_p}} \quad (2.9)$$

Known the value of I_h , from equation 2.7 is possible to evaluate the value V_h . Finally the value of SOC is updated following the expression 2.2.

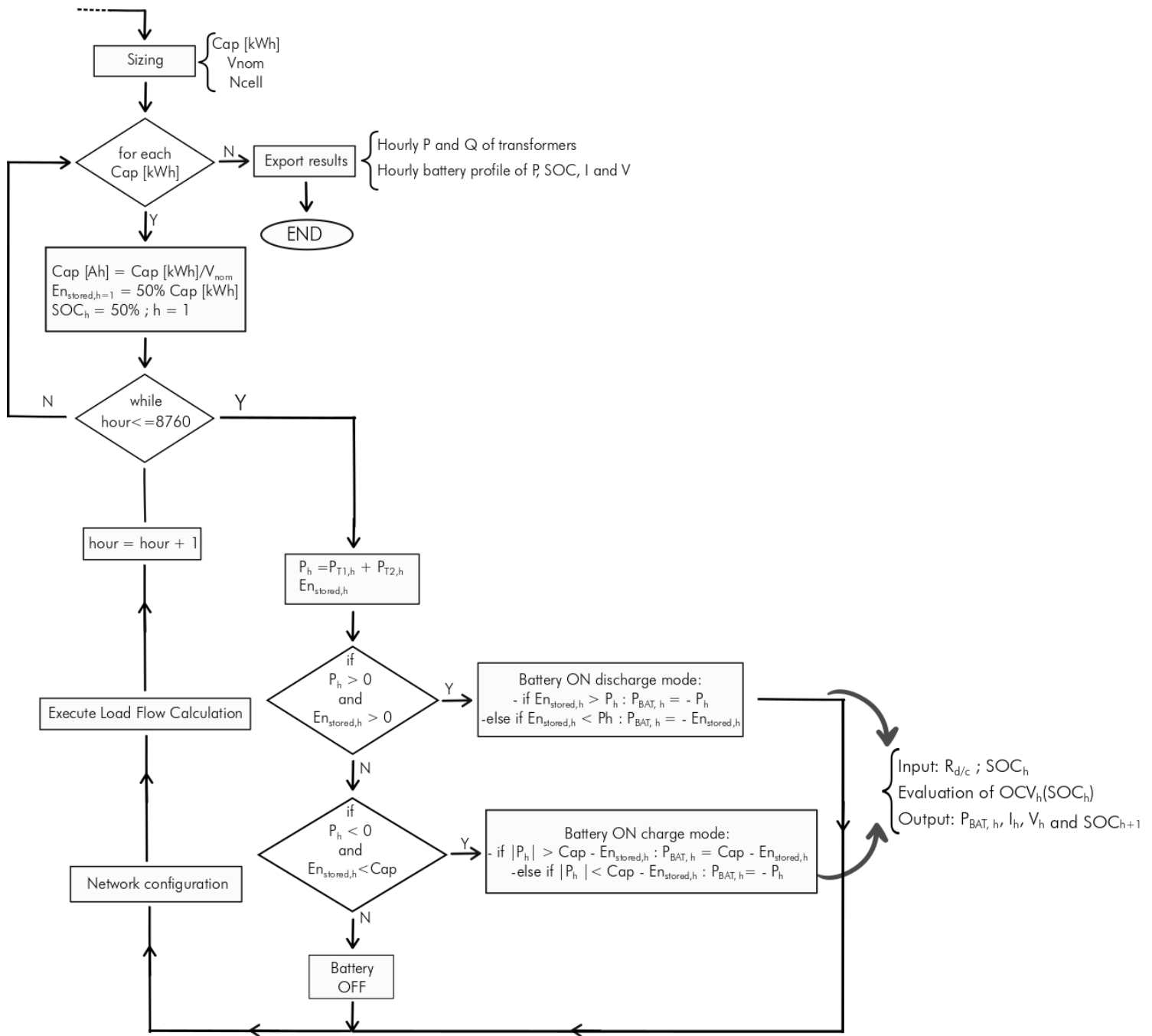


Figure 2.4: Flow chart of the instructions executed in the simulation of the third scenario, model 2. Own elaboration.

2.2 Sizing of the battery

The main services that the battery has to provide to the microgrid are the power supply in case of fault (UPS) in the transmission system and the increase of self-consumption and of the capability of being independent from the main grid. These aspects are decisive in the assessment of the energy capacity of the battery: knowing the hourly electricity demand of the grid, the size of the battery can be calculated as the amount of energy needed to cover consecutively the load demand for a certain time interval. The duration of this time interval has been chosen on the basis of the considerations about the reliability of rural microgrids in Spanish electricity system, expressed in section 1.1, and of the consumption and generation profiles of the grid under investigation.

As consequence of the analysis of the reliability of Spanish rural grids, the minimum time interval during which the battery should be able to operate covering the electricity needs of the grid is equal to two hours, i.e. the TIEPI related to this field. The choice of sizing the capacity of the battery for an higher operating time, as previously told, derives from the analysis of the needs and of the excess in power generation of the grid. The power profile used is the one related to the net power exchange between the microgrid and the external grid in the condition with high PV penetration. Following the aim of minimizing the electricity required from the main grid, the battery is sized in order to cover the load needs during the hours in which there is not PV generation.

The methodology used to quantify the amount of storage capacity needed to provide electricity continuously for a certain time interval is based on the evaluation of the duration curves of the net load required by the grid. A traditional load duration curve shows the load values sorted in descending order so that the maximum value of the curve represents the threshold load that is never overcome during the year (in 0% of cases). Following the same line of reasoning, each point of the curve, identified by an ordinate equal to the load value and an abscissa equal to the occurrence frequency of that load, have to be read as the load value Y that is exceeded in X% of cases during the year.

For the proposed analysis a slightly different approach is used: 24 duration curves are built summing load values included in a range of growing amplitude (from 1 up to 24) and sorting the obtained values in ascending order. In these curves the maximum values corresponds to the maximum amount of energy required in a time interval of n-hours. Setting the battery capacity equal to the these values means that in 100% of the cases the microgrid can be self-sufficient, i.e. fed by the pv generation and by the battery, for at least n-hours. In section 3.1.4 are shown the duration curves obtained for the case object of investigation.

The configuration of the grid that includes the industrial load could presents some issues respect to the application of this method and could require a different approach. If the PV generation, that in this work has been sized in order to respect what prescribed by the law for the constitution of a jointly acting self-consumption community, is not high enough the result would be a battery with a too high capacity that never reaches the condition of full charge. In this case the battery capacity can be evaluated on the basis of the PV generation. On the same duration curve, the lower values, that have a negative sign because are the amount of power that the transformers inject into the external grid, represent the amount of generation surplus produced in a time interval of n-hours. Thus, the lowest value on the curve is the maximum electricity surplus generated and that is never overcome during the year, while a generic Y (negative) value corresponds to the amount of electricity surplus that is overcome in X% of the cases in which the net balance of the grid result negative.

In order to completely define the size of the battery is necessary to determine the nominal voltage, useful to express the energy storage capacity in Ah, and the number of cells. The total number of cells is given by the product between the number of strings, i.e. groups of cells connected in parallels, times the number of strings connected in series: realizing the

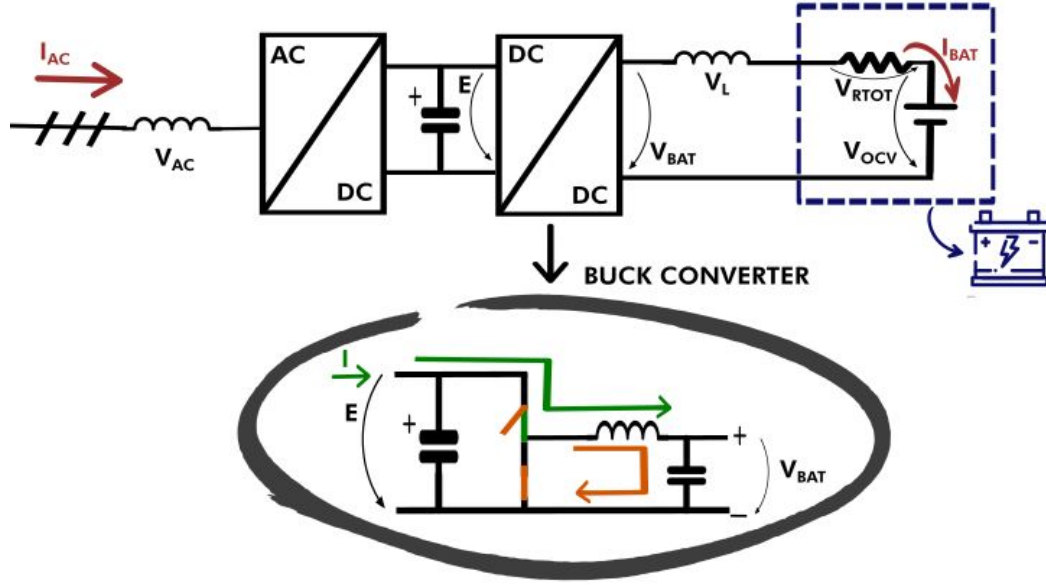


Figure 2.5: Schematic of the electric circuit formed by a battery connected to the AC grid in charge mode. Own elaboration.

appropriated connections is possible to make the battery able to sustain a certain values of voltage and current that can guarantee the required power generation or absorption. These parameter are calculated considering a sample cell of which are known the parameters summarized in table 2.1.

Capacity rating (mAh)	Nominal current $I_{nom,cell}$ (A)	Cut-off OCV (V)	Charge resistance (Ω)	Discharge resistance (Ω)
2000	2	4,2	0,2648	0,2430

Table 2.1: Characteristics of a $LiFePO_4$ sample cell. Source [11]

The capacity, the nominal current and the cut-off open circuit voltage are taken from the CALCE Battery Research Group data [11]. The values of the charging and discharging internal resistance are calculated through a “low-current OCV” test by which has been derived also the linear expression of OCV as function of SOC.

In order to evaluate the voltage at the battery node and the number of cells is necessary to consider the whole system included between the battery and the AC-grid. As shown in figure 2.5 the components taken into account are the 3-phase grid, the AC/DC converter, the DC/DC converter and the battery. The voltage at the AC side is 400 V and is converted into the line voltage E , at the DC side, equal to 653,2 V. From the simulation performed following the battery model 1 is possible to find out which is the most stressful working condition of the battery, that corresponds to a maximum injected power in charge mode ($P_{max_{charge}}$).

The DC/DC converter has to be sized, in terms of duty cycle and output voltage, in order to be able to sustain the same power condition of the battery. Choosing the value of the duty cycle equal to 0,95, the DC/DC link, that in charge mode is a buck converter,

performs a step down voltage reduction:

$$E = \frac{2\sqrt{2}}{\sqrt{3}} V_{AC} = 653,2V \quad (2.10)$$

$$d = 0,95 \quad (2.11)$$

$$V_{BAT} = d \cdot E = 620,5V \quad (2.12)$$

V_{BAT} is the voltage at the output of the buck converter, on the battery side. Between the output nodes of the converter and the battery an electric circuit is formed. The circuit is composed by the battery, modeled as a voltage source (V_{OCV}) and a total internal resistance (R_{tot}), an inductance, which is associated a null inductive voltage drop and a Ohmic resistance (R_l), and is closed by the buck converter voltage output (V_{BAT}). V_{ocv} (eq. 2.13) and R_{tot} (eq. 2.14) are respectively the equivalent voltage and resistance of the battery.

$$V_{OCV} = N_s \cdot OCV \quad (2.13)$$

$$R_{tot} = R_{ch} \frac{N_s}{N_p} \quad (2.14)$$

where N_p is the number of cells connected in parallel, forming a string, and N_s is the number of strings connected in series. The current (I) flowing in the circuit is the same that flows across the DC/DC converter:

$$I = P_{max\,charge} \cdot V_{BAT} = 65A \quad (2.15)$$

from which is possible to calculate N_p , equal to

$$N_p = \frac{I}{I_{nom,cell}} \quad (2.16)$$

Applying the Kirchhoff Voltage Law is obtained the following expression:

$$V_{BAT} - R_{tot} \cdot I - V_{OCV} = 0 \quad (2.17)$$

and substituting the terms previously expressed,

$$V_{BAT} - R_{ch} \frac{N_s}{N_p} I - N_s \cdot OCV = 0 \quad (2.18)$$

from which is calculated N_s

$$N_s = \frac{V_{BAT}}{\frac{R_{ch} \cdot I}{N_p} + OCV} \quad (2.19)$$

The nominal voltage of the battery is :

$$V_{nom} = N_s \cdot OCV + R_{ch} \frac{N_s}{N_p} I \quad (2.20)$$

The capacity of the battery can be expressed in Ah as the ratio between the value of capacity measured in kWh and the nominal voltage of the battery.

2.3 Economic Analysis

The economic analysis develops on three steps: the calculus of the yearly electricity bills for the jointly acting self-consumers group for all the scenarios of consumption, the evaluation of the savings obtained with the installation of only PV power systems and with both PV systems and the battery and, in the end, the assessment of the feasibility of the investment calculating the Net Present Value (NPV) and the Pay Back Time (PBT).

2.3.1 Electricity bills

For the first scenario only the purchase of electricity is considered. Since we are interested only in the jointly acting self-consumption participants, the factory's bills are not taken into account in any scenario, while the residential bills are calculated applying the VPSC tariffs to the hourly energy consumption measured for each load.

In the scenarios in which self-consumption and distributed electricity production is realized, the evaluation of the electricity bills of the prosumers has to consider both the purchase and sell of electricity. The subjects directly involved in this economic interactions are, in all the cases, the jointly acting self-consumption community and the Distributor but all the electricity exchanges have to be taken into account in the different grid configurations.

Configuration without the factory

In this case all the prosumers are part of the jointly acting self-consumption community and, in absence of a storage system and of other consumers within the grid to which sell the surplus of the electricity produced, they can only realize self-consumption and sell the electricity in excess to the Distributor, injecting it into the external grid. The hourly bill are calculated applying the VPSC tariff, when the net load consumption is positive, and the intraday cost of electricity, when the net load consumption is negative, as prescribed by the "Simplified compensation mechanism". When the battery is included into the grid, it is necessary to consider that part of the consumption is covered by the electricity stored into the battery, as well part of the excess of electricity is not sold but stored. Thus, instead of measuring the amount of electricity consumed and produced by each prosumer through the smart-meters installed in each load site, the whole grid net electricity need is considered, measuring the amount of power crossing the transformers. When the net power exchange ($P_{transformers_h}$) is positive the whole grid electricity expenditure is calculated applying the VPSC tariff and the relative bill ($Expenditure_{h,i}$) is allocated to each consumer with its β coefficient.

$$Expenditure_{h,i} = \beta_i \cdot P_{transformers_h} \cdot \Delta t \cdot VPSC_h \quad (2.21)$$

When the net power across the transformer is negative, the income for the whole community is calculated applying the intraday cost of electricity and the distribution of the income is done through the α coefficient.

$$Revenue_{h,i} = \alpha_i \cdot P_{transformers_h} \cdot \Delta t \cdot C_{intraday_h} \quad (2.22)$$

In both the expressions the time interval (Δt) is equal to 1 hour. The hourly bill for each prosumer is calculated as the difference between the hourly expenditure and revenue. Then, an invoicing period of one month is considered and if, for each prosumer and during each invoicing period, the economic value of the electricity sold results higher than the one of the electricity consumed, the relative bill is posed equal to zero.

Configuration with the factory

The factory acts as a load within the microgrid that doesn't participate to the self-consumption. For this reason is necessary to consider the revenues due to the sale to the factory of the excess of electricity produced by PV systems and of the electricity injected by the battery.

As previously said, who is directly involved in the economic interactions are the prosumers and the Distributor. In this way all the electricity injected into the internal distribution grid, both if used to feed the factory and to the back-feed the external grid, can be considered sold by the jointly acting self-consumers to the distributor. Thus, the electricity bills in the case without storage are evaluated considering the net load consumption profile of each consumer and applying the relative tariff.

In the scenario with the battery is necessary to distinguish the different contributions to the incomes because the excess of electricity is not only sold to the distributor. The hourly bill for each prosumer can be considered as the results of four voices: the hourly expenditure (I), the revenues obtained feeding the factory with the electricity stored in the battery (II) or with the excess of PV production (III) and the ones due to the sale of electricity to the distributor (IV) (eq. 2.23).

$$Bill_{h,i} = Expenditure_{h,i} - Revenue_{factory\ h,i} - Revenue_{battery\ h,i} - Revenue_{Distributor\ h,i} \quad (2.23)$$

The expenditure is calculated when the net power across the transformers is positive, with the following expression

$$Expenditure_h = (100 - \%factory_{cons_h}) \cdot Ptransformers_h \cdot \Delta t \cdot PVPC_h \quad (2.24)$$

where

$$\%factory_{cons_h} = \frac{Pfactory_h}{Ptransformers_h} \cdot 100 \quad (2.25)$$

Then the allocation to each consumer is give by

$$Expenditure_{h,i} = \beta_i \cdot Expenditure_h \quad (2.26)$$

The income relative to the sale of PV excess generation to the factory is obtained estimating the amount of electricity sold as the difference between the total electricity surplus, the amount of electricity stored in the battery (if the battery is in charge mode) and the amount of electricity injected into the external grid (if the power across the transformers measured is negative)(eq. 2.27).

$$Revenue_{factory\ h} = \left[\sum_i NetLoad_{h,i} - Pbattery_h - Ptransformers_h \right] \cdot Cintraday_h \quad (2.27)$$

If the battery is not charging or there is not back-feeding the second and third terms of eq. 2.27 are null respectively.

The income relative to the amount of electricity consumed by the factory when the microgrid is fed by the battery is calculated as

$$Revenue_{battery\ h} = \%factory_{cons_h} \cdot Pbattery_h \cdot Cintraday_h \quad (2.28)$$

The last term, relative to the income due to back-feeding, is calculated as

$$Revenue_{\text{Distributor } h} = P_{\text{transformers}_h} \cdot C_{\text{intraday}_h} \quad (2.29)$$

Finally, the revue for each prosumer is calculated using the α coefficient:

$$Revenue_{\text{factory } h,i} = \alpha_i \cdot Revenue_{\text{factory } h} \quad (2.30)$$

$$Revenue_{\text{battery } h,i} = \alpha_i \cdot Revenue_{\text{battery } h} \quad (2.31)$$

$$Revenue_{\text{Distributor } h,i} = \alpha_i \cdot Revenue_{\text{Distributor } h} \quad (2.32)$$

Then, the bills are estimated for invoicing periods of one month and are posed equal to zero if the revenues overcome the expenditures.

2.3.2 Savings

For each prosumer and then for the whole joint acting self-consumers group, the yearly bill is calculated. Comparing the values obtained in the case with only high PV penetration and in the case with the battery with the one of the base case is possible to evaluate the economic savings generated.

2.3.3 Discounted cash flow analysis

The evaluation of the NPV and of PBT is based on the discounted cash flow analysis. This is a very diffused methodology for the assessment of an investment in energy sector. This method allow to evaluate the convenience of the investment taking into account the time value of money of the future cash flows and the financial structure adopted. A key role, in discounted cash flow analysis, is played by the discount rate chosen that has to be at least equal to the rate of return of a risk-free investment but has to consider also the inflation, i.e. the loss of purchasing power of money during the whole life time period of the project, and an additional premium for the assumption of the investment risk. The discount rate can be chosen equal to the weighted average cost of capital (WACC) that gives a measure of the rate of return of the capital cost of the project based on the shared percentage of equity and debt, i.e. on the financial structure of the investment. To choose what financial structure adopt for an investment in energy field is possible to follow the guidelines suggested by the NETL methodology in the document “Quality guidelines for energy system study - Cost Estimation Methodology for NETL Assessment of Power Plant Performance” [28]. In this document are expressed common values of the percentage and of the cost of equity and of debt (E and c_E , D and c_D respectively) for scenarios affected by different levels of risk. This values, both with the country tax rate (t), are used to calculate the WACC with the formula

$$WACC = E \cdot c_E + D \cdot c_D(1 - t) \quad (2.33)$$

The tax rate of the country in which the investment is realized can be found in the Deolitte Corporate Tax Rates [29] and is equal to 25% for Spain (in 2019).

The discount rate, here indicated with letter i and that will be set equal to the WACC, is used to calculate the present value (PV) of a future cash flow (B), occurring n years after the current year, following the expression

$$PV = \frac{1}{(1 + i)^n} B \quad (2.34)$$

In the case of a series of future cash flows, the present value is

$$PV = \sum_{y=1}^n \frac{B_y}{(1+i)^y} \quad (2.35)$$

where n is the duration, expressed in number of years, of the time period in which the cash flows occur. If the series of cash flows correspond to a uniform series of payments or incomes the expression of the present value becomes

$$PV = \frac{(1+i)^n - 1}{i(1+i)^n} B \quad (2.36)$$

A present value of cash flow that results particularly interesting in the economical assessment of a project is the Net Present Value (NPV), which expression allows to evaluate also the Pay Back Time of the investment. The NPV takes into account both expenditures and incomes, considered as negative and positive cash flows respectively. The initial expenditure is represented by the project capital cost, i.e. the CAPEX. For the analysed project it results being the sum of the cost of the installation of the PV panels, calculated as the cost per kW of a PV power system times the total installed power, and of the cost of the battery. The investment cost of the installation of the PV power systems is estimated on the basis of the recent trends, as reportend in the document [30]. The cash flows that occur after the start-up of the project are named operational costs (OPEX). To this set can belong incomes related to the direct sale of the electricity produced or related to the money savings with respect to the previous economic consumptions. Since the Royal Decree 244/2019 [27] foresees that the economic value of the electricity generated can't exceed the one of the electricity consumed, only savings are taken into account. Also operational and maintenance costs (OM), usually estimated as a percentage of the initial investment, and subsidies would be part of OPEX: both this cash flows are not considered in the case under investigation since maintenance cost for PV panels and Lithium battery can be neglected and subsidies are not actually supplied in Spain.

To evaluate the yearly cash flow is necessary to consider also the effect of the country tax rate (in case of generation of positive cash flow) and of the depreciation. The formula used to evaluate the yearly cash flows is

$$Cashflow_y = Savings_y - t(Savings_y - Depreciationrate) \quad (2.37)$$

where the depreciation rate is calculated as the ratio between the total investment cost and the depreciation time. It is applied since the year that follows the one in which the investment is realised and only during the depreciation time: in this way, in the year "zero" the cash flow is equal to the investment and after the depreciation time period the taxes are evaluated considering only the incomes, setting the depreciation rate equal to zero in the previous expression. Then, applying the discounted rate, the expression of the NPV results being the following

$$NPV = -Investment + \sum_{y=1}^n \frac{Cashflow_y}{(1+i)^y} \quad (2.38)$$

Solving this equation with respect to the number of year, imposing a null NPV, means find the PBT, i.e. the time necessary to recover the investment and start in generating revenues. In fact, once overcome the year related to the PBT, the NPV passes from being negative to positive. In order to assess in a favorable way the economic feasibility of the investment proposed, the PBT has to correspond to a reasonable number of years, also with respect to the life time of the technologies involved.

Emisiones y factor de emisión de CO ₂ asociado a la generación de energía eléctrica nacional										
	2008	2009	2010	2011	2012	2013	2014	2015	2016	2017
Carbon	44.182.945	33.053.374	22.515.583	41.103.360	51.122.747	37.551.186	41.154.288	50.149.589	35.616.709	42.936.455
Fuel/gas	8.222.911	7.683.629	7.321.668	6.057.486	6.116.754	5.491.082	5.102.790	5.257.557	5.491.480	5.695.781
Ciclo combinado	35.538.149	30.729.259	25.826.072	21.049.929	16.460.886	11.547.529	10.635.491	12.154.925	12.069.345	15.036.167
Térmica renovable	450.753	517.529	539.206	728.423	806.845	861.146	802.056	0	0	0
Cogeneración	9.871.389	10.568.296	11.440.743	11.929.272	12.463.954	11.921.983	9.546.802	9.416.313	9.585.446	10.423.065
Residuos	0	0	0	0	0	0	0	791.558	814.167	836.321
Total Emisiones (tCO₂)	98.266.148	82.552.086	67.643.272	80.868.470	86.971.186	67.372.926	67.241.427	77.769.941	63.577.147	74.927.789
Factor emisión (tCO₂/MWh)	0,332	0,295	0,234	0,289	0,307	0,246	0,252	0,294	0,242	0,285

Figure 2.6: CO₂ emissions and CO₂ emission factor of the Spanish electrical generation park. Source [8]

2.4 Environmental impact

The environmental impact generated by the execution of this project is evaluated through the Carbon footprint associated to the technologies involved, the PV panels and the LiFePO₄ battery, and to the new grid's electricity demand.

Carbon footprint of the grid

The environmental benefit generated covering a large part of the grid needs with RES production and with the battery is measured in terms of Carbon footprint of the grid. Since in this work is not foreseen the replacement or the decommissioning of power plants and generators that produce other pollutants, only CO₂ is considered.

The CO₂ footprint is calculated on the basis of the yearly energy consumption of the grid, measured as the total amount of electricity absorbed from the transmission system. In order to estimate the amount of CO₂ associated to the electricity consumed and generated by the grid, the CO₂ emission factor is used. This factor expresses the ton of CO_{2-eq} associated to each MWh produced. It's evaluated at national level on the basis of the emissions generated by all the power plants that produce CO₂ and, as shown in table 2.6, in Spain in 2017 it was equal to 0.285 tCO_{2-eq}/MWh [8].

Comparing the results obtained for the scenarios with high PV penetration and with the battery with the base case is possible to have an estimation of the percentage decrease of emissions.

Carbon footprint of PV systems

The Carbon footprint linked to the production of a Silicon (Si) PV system is estimated in terms of grams of CO₂ equivalent emitted per kWh produced during the whole life time of the system, considered equal to 30 years. These virtual emissions allow to quantify the CO₂ effectively generated during the life cycle of these technology from "cradle-to-grave", i.e. from the extraction of the raw materials to the disposal. As represented in figure 2.7, between these two extreme steps there are several phases that have to be considered in the Life Cycle Assessment (LCA): the energy required in the material processing and purification, aimed to reach the solar-grade purity, the manufacturing processes, from the ingots to the complete PV system, the use, the decommissioning, the transport of materials between each phase, and the eventual recycle. The higher amount of CO₂ emissions are generated during the material processing and during the manufacturing of the PV modules (figure 2.8). In these phases the Carbon footprint is associated to the electrical and thermal energy consumed, considering the emission factor of the national electricity generation park.

For this reason the Carbon footprint of the PV systems production is strictly linked to the country in which is produced and to its electricity supply mix.

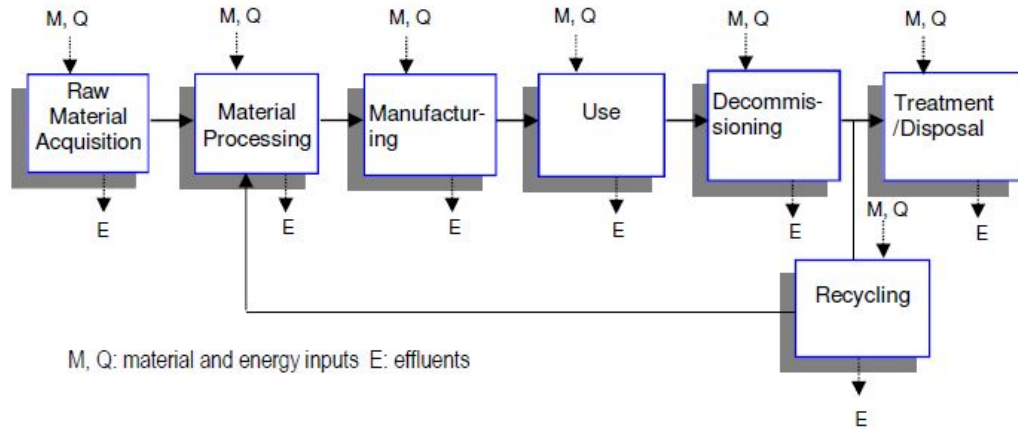


Figure 2.7: Life cycle stages of a PV system. Source [9]

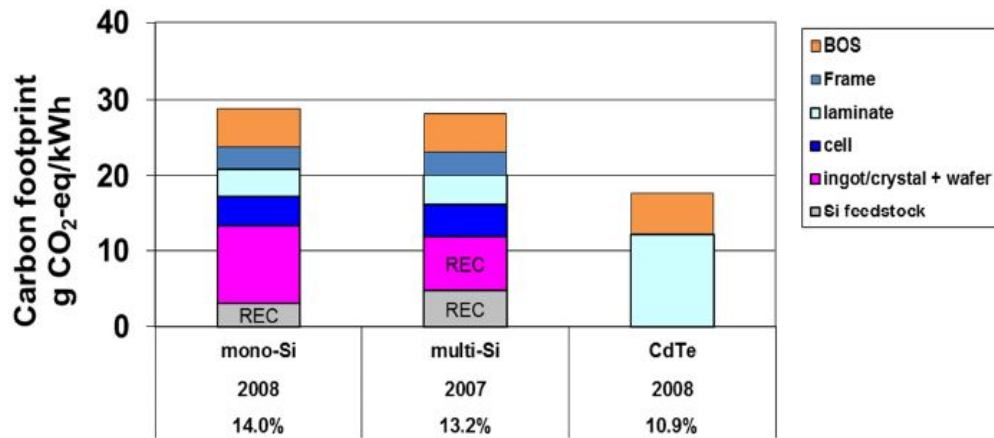


Figure 2.8: Life cycle Greenhouse Gases (GHG) emissions from rooftop mounted PV systems produced and installed in a Southern European country. Source [9]

For a mono-Si rooftop PV system characterized by a performance ratio of 0.75, produced and installed in a Southern European country, which presents a solar irradiation of 1700 kWh/m²/yr and considering a lifetime of 30 years, the Carbon footprint is around 29 g of CO_{2-eq}/kWh. As reported in the document [9], from which figure 2.8 is taken, this value considers also the CO₂ generation associated to the aluminium frame production, and to the other elements of the Balance of System (BOS), that in the case of a rooftop PV system are inverters, mounting structures, cable and connectors. Besides, this value is coherent with the ones reported in other publications as de Wild-Scholten [31] and Fthenakis et al. [32].

This assessment of the Carbon footprint doesn't include the recycle processes that is demonstrated having a positive net environmental impact: the emissions, not only of CO₂, generated during the processes of materials recovering are lower that the ones generated for the production or extraction of new primary materials [33]

Carbon footprint of the battery

Concerning the battery, in literature there are several results of LCAs studies that express the GHG emissions relative to the batteries production processes. This is mostly due to the different approaches used in the LCAs studies.

In this work is considered the value corresponding to the average result of the review conducted by Peters et al. (2017) [34]. The Carbon footprint associated to the production of a LiFePO_4 battery is considered equal to $161 \text{ kgCO}_{2\text{-eq}}/\text{kWh}$, with respect to the battery capacity.

Also for the battery is possible to execute the recycle of materials, both of the pack and of the cell. The first case involves materials like aluminium, steel and copper that already know a well developed recycle chain. About the cell materials two technique are currently used: the Pyrometallurgy and the Hydrometallurgy, for the recover of cobalt, nickel, copper and in some case iron. Although the recycle of these materials is very important in order to limit the consumption of the materials themselves, from an energetic and environmental point of view these technique have not a positive impact on the LCA of the battery: the Pyrometallurgy adds further GHG emission to the life cycle of the battery, while the Hydrometallurgy generate a very small reduction [35].

Chapter 3

Study Case

The proposed methodology for the study of a rural microgrid characterized by an high renewable penetration and by the presence of a battery energy storage system has been applied to the study case described in this chapter. In section 3.1 the description of the grid is provided. In section 3.2 are illustrated the scenarios object of the simulations conducted. Section 3.3 shows the obtained results concerning the battery and the transformers behaviour, the economic feasibility and the environmental impact of the project.

3.1 Description of the microgrid

The microgrid under investigation is located in Santa María de Corcó, in Girona. Figure 3.1 shows an areal picture of the location in which the sites highlighted with red circles are the two electric substations (SSs), named SS 030 and SS 528.

In the substations are installed two transformers that realize the connection with the transmission grid and from which the radial distribution network develops. It is a LV distribution network (at 400 V) that feeds 21 loads. Loads 1÷20 are residential loads, characterized by a contracted power lower than 10 kW. Because of a lack of availability of data, loads 7, 9, 14, 18 are not included in the simulations. Besides in 4 houses, corresponding to load 16, 17, 19 and 20, PV systems are really installed. Load 21 is a factory and is characterized by a very different consumption with respect to the other loads. In the following paragraphs a more detailed description of the elements of the grid here mentioned is given.

3.1.1 Transformers

Both the transformers are three-phase winding transformers Yy connected on the HV side to the transmission grid at 690 V and on the LV side to the 400 V distribution grid. The transformers with the highest apparent nominal power is installed in SS 030, that is the one that feeds the part of the grid including the factory. The technical features of the transformers are summarized in table 3.1.

The terminals and the cables

The microgrid includes 32 terminals which operating condition is defined only setting the nominal voltage. For all the terminals that are located within the grid the voltage is set at 400 V while terminals 31 and 32, that are located on the HV side of the transformers, are set at 690 V. Terminal 1, that represents the SS 030, is the terminal to which the battery will be connected in the simulations. The terminals and the loads are connected trough 31

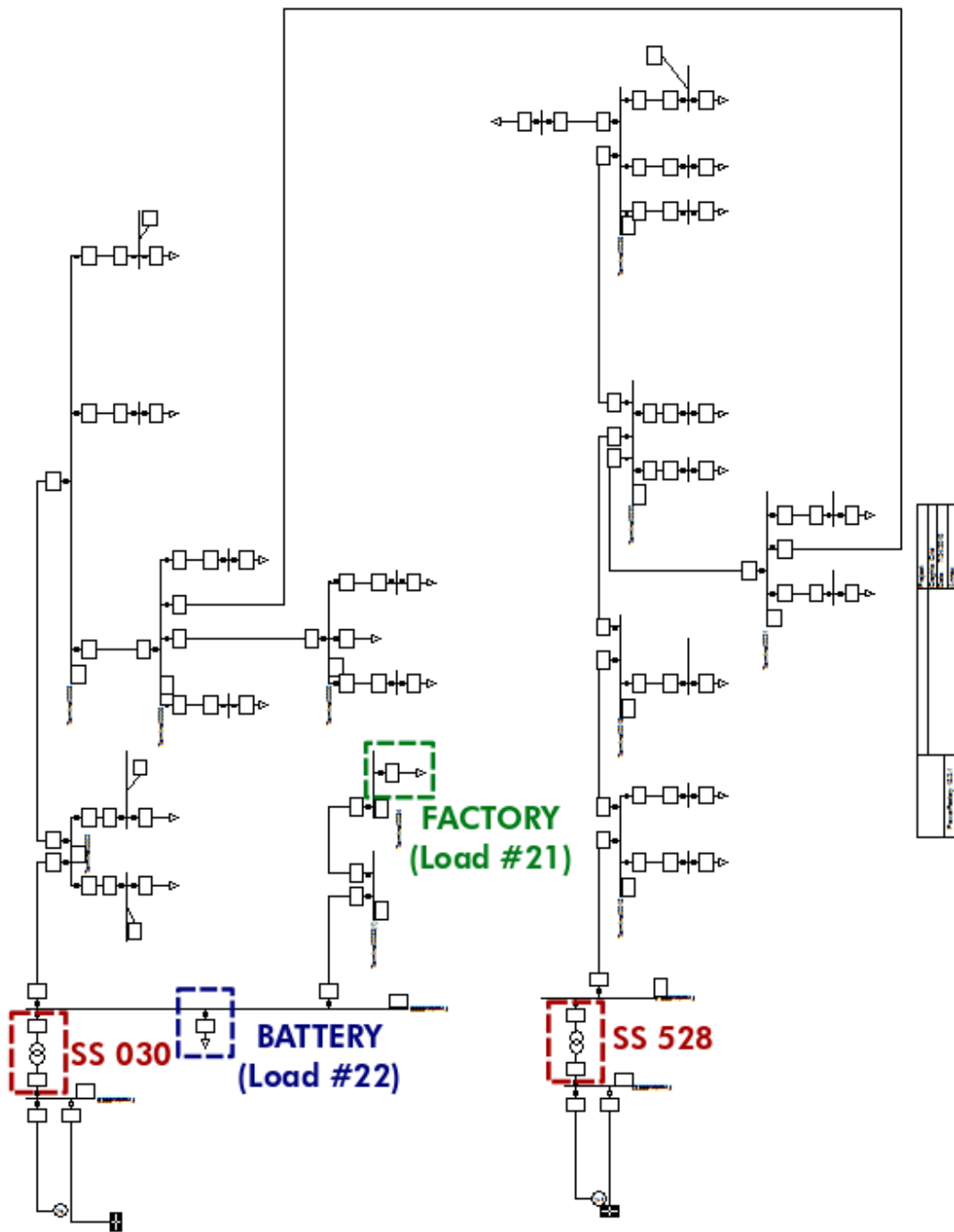


Figure 3.2: Diagram of the microgrid obtained from DigSILENT.

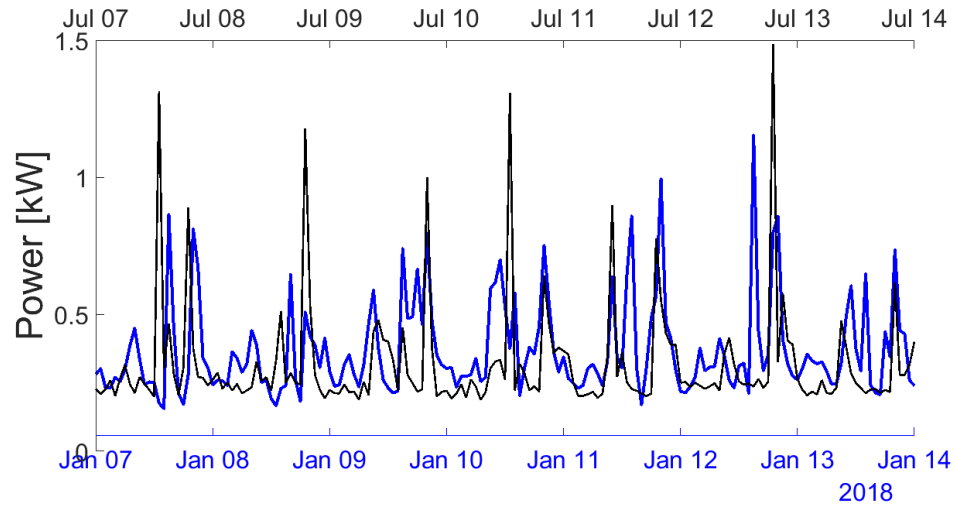


Figure 3.3: Comparison of the weakly evolution of the consumption of load 11 during winter (blu line) and summer (black line).

the reliability of the grid in case of fault in one of the two substation. In the simulation this line has been considered yet installed: in this way the battery, which proposed location is in SS 030, can feed both side of the network. The length, the section, the resistance, the inductance and the phase voltage are the parameters required to define the behaviour of the cables in the simulation.

3.1.2 Residential loads and PV systems

The residential loads are characterized by an installed power lower than 10 kW. They cumulatively generate a peak power of 26 KW and a yearly consumption of 76 MWh. They are equipped with smart meters that are able to measure the active and reactive power required by each consumer every hour. For each consumer, therefore, is known the hourly consumption profile during a year. Figure 3.3 shows the weakly profile of a load (load 11), with a contracted power of 3 kW, in winter (blue line) and in summer (black line). The winter profile shows three daily peaks, around 8:00 in the morning, 3:00 and 9:00 in the evening. The summer profile shows only two peaks of power demand, around 1:00 p.m. and 7:00 p.m.. The maximum and minimum power required in the two periods are quite similar but the consumption results higher during winter: between January and March 832 kWh are consumed, while between June and August the consumption decrease to 720 kWh. The behaviour of the other loads is quite similar and therefore also the whole grid consumption has the same trend, with a winter consumption of 20 MWh against 15,6 MWh during summer. These value are referred only to the residential loads.

In load 16, 17, 19 and 20 PV systems are installed. In table 3.2 are summarized the values of the peak power and of the yearly producibility of the PV systems, obtained from the available data. In fact, also for the PV systems the hourly power generation is measured and there are available values for a period of one year.

Figure 3.4 shows the weakly profile of the PV generation of the PV system installed in load 16 (dropped line), that is the one with the higher peak power and prouducibility, and the one of the PV system installed in load 20 (continuous line), that on the opposite has the lower peak power. Also in this case the comparison is between the winter and the summer period, resulting, in this case, in an higher summer generation.

Installed in:	Load 16	Load 17	Load 19	Load 20
Peak Power (kW)	6,5	4,6	4,3	3,5
Yearly producibility (MWh)	10,6	6,9	7,4	5,5

Table 3.2: Peak power and yearly producibility of the PV systems installed in load 16, 17, 19 and 20.

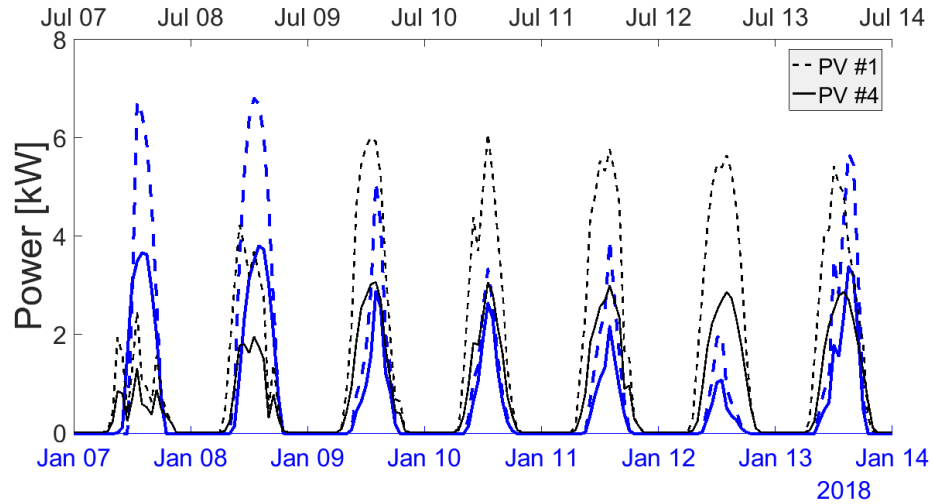


Figure 3.4: Comparison of the daily evolution (for one week) of the power generated by the PV system installed in load 16 and in load 20, during winter (blue line) and summer (black line).

Considering again the load 16, the net consumption profile, resulting from the difference between electricity consumed and generated, has a daily evolution of the type shown in figure 3.5. What is evident is a deep valley in the curve of the summer day, during the hours of PV production, that represents the amount of electricity that exceed self-consumption and can be injected into the distribution grid.

3.1.3 Factory

The factory represents the main contribution to the grid consumption: the active power required is between 20,7 kW and 62,1 kW and the yearly consumption is about 320 MWh, 4 times the yearly consumption of the residential loads. Its consumption profile is regular during the year, as shown in figure 3.6. Also the consumption of reactive power is significant, around 16 MVarh/year, and could compromise the grid generating not admissible voltage drops.

3.1.4 Battery

The model of battery chosen, for the reasons described in section 1.2.4, is a Lithium Iron Phosphate battery (LiFePO_4), provided by Fenecon [10]. The technical specification are summarized in the following table.

How is possible to see from the model shown in figure 3.7, this battery has a modular

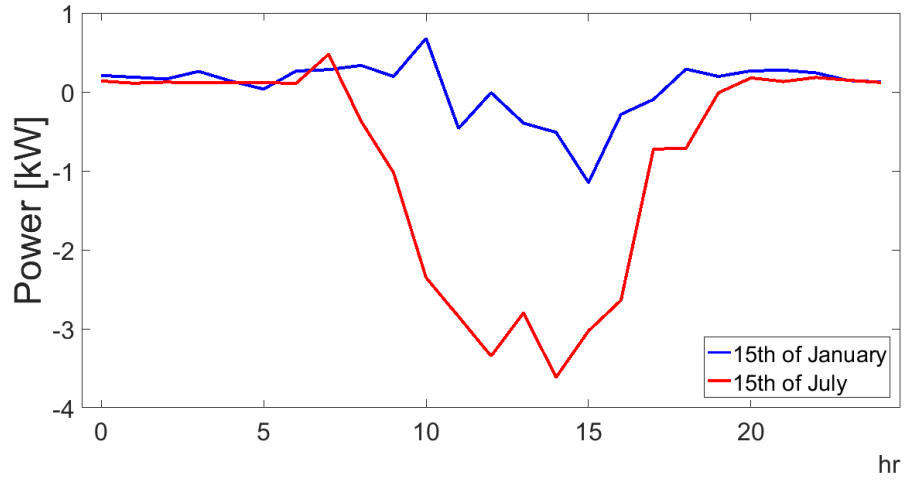


Figure 3.5: Comparison of the net daily profile of load 16 during a winter and summer day.

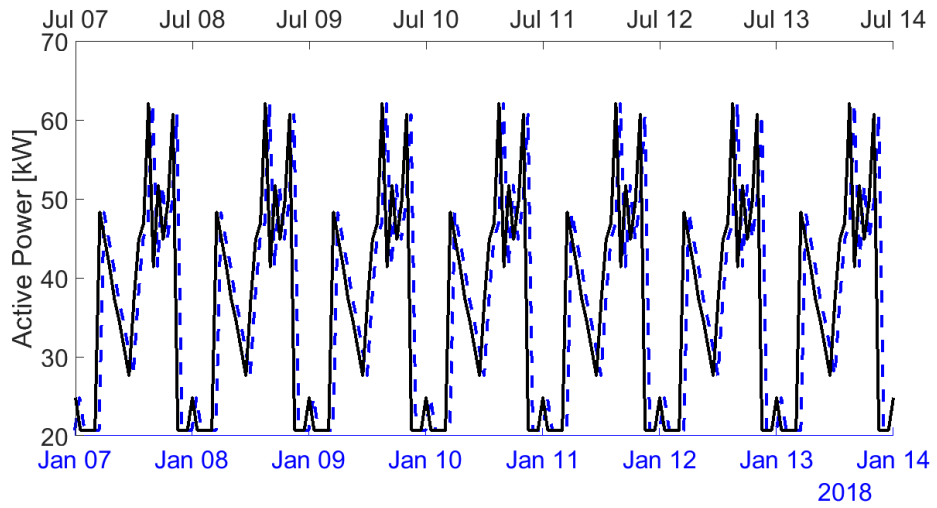


Figure 3.6: Comparison of the daily active power factory consumption profile during winter (blue dropped line) and summer (black line).

Capacity (kWh)	Voltage (VDC)	Max. Current (A)	Temp. range (°C)	Weight (kg)	Size (mm)
50	696 ÷ 854	80	-20 ÷ 55	450	540/540/2200

Table 3.3: Battery features referred to two battery modules, as the ones shown in figure 3.7. Source [10]

structure. Connecting modules in series is possible to increase the capacity, the power peaks and the voltage that the battery can provide. The features listed in table 3.3 are referred to a battery made of 10 modules connected in series. The manufacturer guarantees a conservation of the 70% of the initial capacity after 12 years of operation or 6000 cycles. Besides the battery is provided with a DC/AC inverter characterized by the technical features listed in table 3.4.



Figure 3.7: The battery. Source [10]

Inverter	
Rated Power (kW)	50
Current (A)	3*72.4 A @230V
Frequency (Hz)	50/60
THD	<=1%

Table 3.4: Inverter's features. Source [10]

The steps followed in order to define the capacity of the battery are the ones described in section 2.2. At first the grid consumption, of a scenario with an high PV penetration that will be described in section 3.2, has been analyzed. The choice of sizing the battery in order to cover continuously the grid needs for 6 hours appears reasonable. In the grid configuration without the factory this time interval is referred to the hours between 6 p.m. and 12 p.m., when the demand is higher and there is not PV generation (fig. 3.8). The battery is aimed to replace the external grid in covering this part of the grid consumption. Besides, this choice is coherent with the reliability analysis of the Spanish rural grids.

Then the duration curves, represented in figure 3.10 and 3.12, have been built, with the methodology previously described. The highlighted curves refer to the amount of energy required to cover continuously the microgrid's needs for six hours without the supply by the external grid. In the case without the industry is possible to see that this quantity is lower than the maximum surplus of electricity that occurs in a time interval of the same duration (i.e. the lowest value of the curve). This guarantees that will be possible to satisfy the grid requirement and make the battery undergo complete charge and discharge cycles. Figure 3.11 shows the curves representing the values of energy capacity that the battery has to have for covering several numbers of hour in 100%, 95%, 90% and 85% of cases respectively.

The curves relative to the configuration with the factory show an opposite situation: the amount of energy that would be necessary store for the continuous coverage of the grid consumption for 6 hours is higher than the maximum surplus generation. A battery with a capacity of 360 kWh would be necessary, but the maximum surplus is only of 177 kWh. For

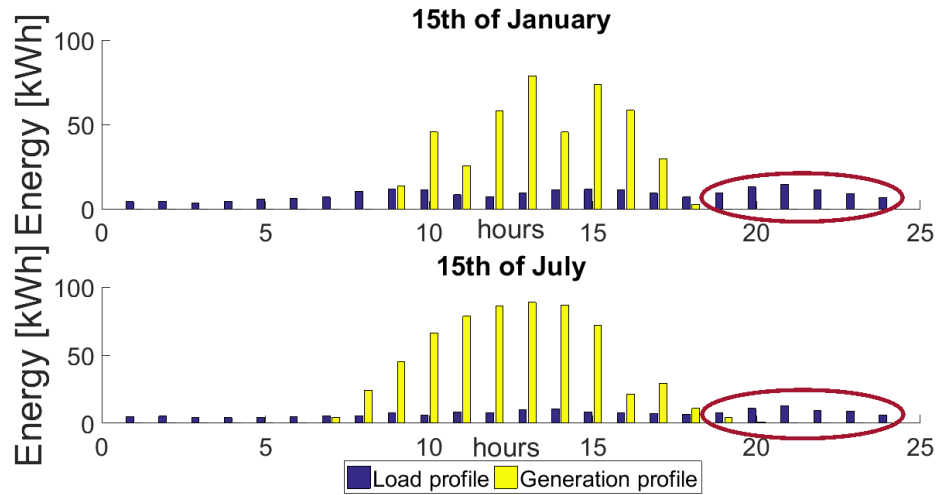


Figure 3.8: Comparison between the grid generation and consumption profile in a winter (top) and summer (bottom) day, referred to the grid configuration without the factory.

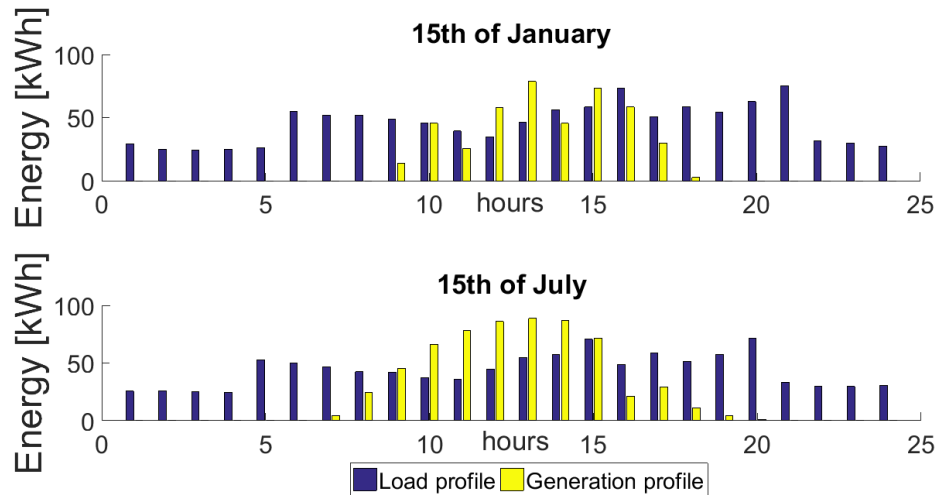


Figure 3.9: Comparison between the grid generation and consumption profile in a winter (top) and summer (bottom) day, referred to the grid configuration with the factory.

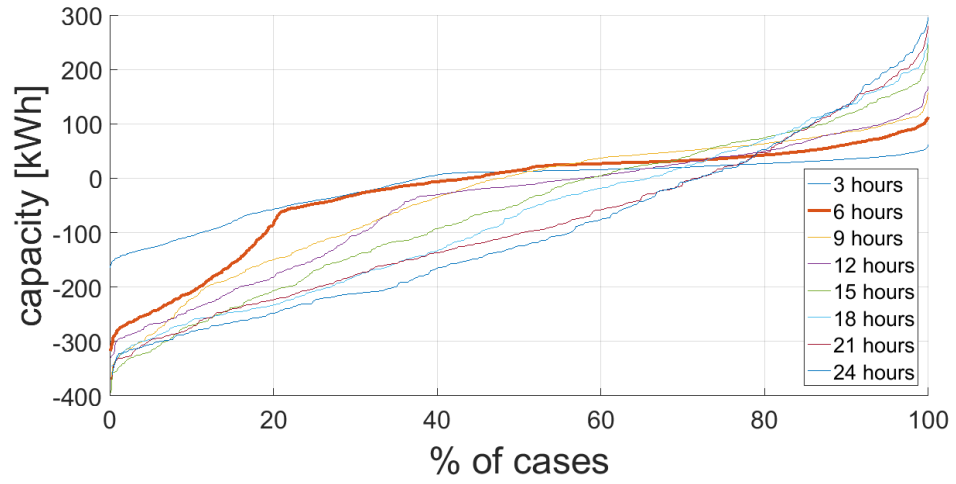


Figure 3.10: Duration curves of the grid configuration without the factory.

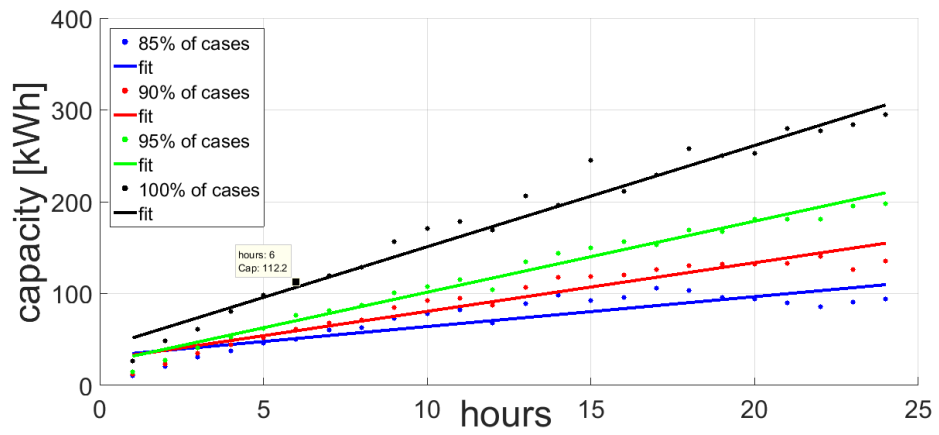


Figure 3.11: Battery capacity required as function of the number of hours during which the grid consumption is covered continuously.

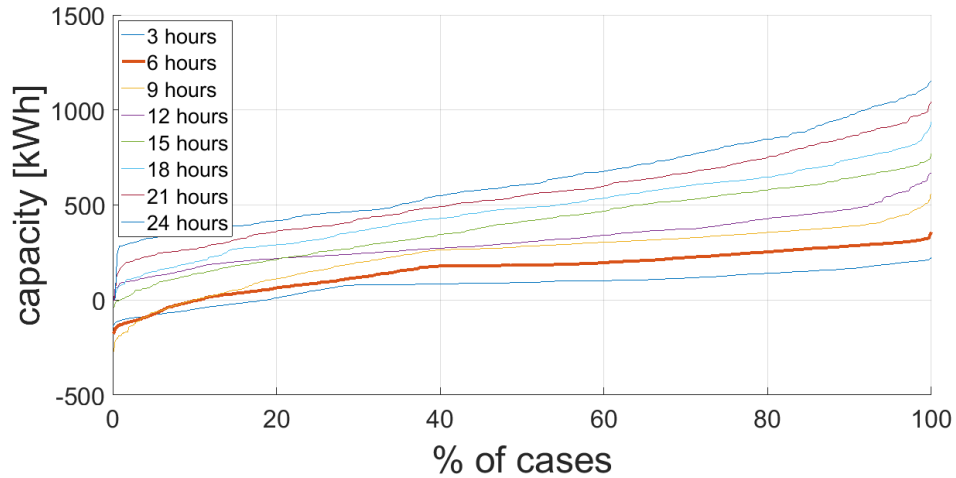


Figure 3.12: Duration curves of the grid configuration with the factory

this reason the capacity is chosen on the basis of the available electricity excess.

In the following tables are summarized the values of battery capacity, in kWh and Ah, and the relative battery nominal voltage obtained. In table 3.5 100%, 95%, 90% and 85% are the percentage of cases in which the associated battery capacity guarantees a complete coverage. In table 3.6 0% and 20% are the percentage of cases in which the PV generation exceeds the value that is chosen as battery capacity.

	Factory not included			
	100%	95%	90%	85%
Nominal Voltage (V)	604	607	607	611
Capacity (kWh)	112	76	62	50
Capacity (Ah)	186	126	105	88

Table 3.5: Battery size calculated for the grid configuration without the factory.

	Factory included	
	0%	20%
Nominal Voltage (V)	585	595
Capacity (kWh)	177	114
Capacity (Ah)	512	454

Table 3.6: Battery size calculated for the grid configuration with the factory.

3.2 Scenarios

The simulations have been conducted for three different scenarios, both in the case in which the industry (i.e. load 21) is not included into the grid and in the one in which it is, considering a time period of one year. The first scenario considers a microgrid in which there is not electricity production from PV power system. The load profile of the loads 16,

17, 19 and 20, in which PV panels are really installed, is modified adding the hourly PV generations of the corresponding installed PV system. In this way will be possible to compare the results of the following scenarios with a condition of absence of self-consumption.

In fact, the second scenario has the aim to simulate the behaviour of a microgrid with an high renewable generation penetration and in which the presence of a storage system is not still included. To each load in which there is not a real PV generation is applied a PV generation profile. A different approach is used between the case without and with the industry. In the first case to each load is applied the generation profile of the PV panel installed in the load with the closer yearly consumption (between load 16,17,19,20). The resulted total PV installed power is of 67,7 kW. In the second case, in order to maximize the self-consumption of the grid, to almost all the loads is applied the generation profile of the generator with the highest yearly producibility (i.e. the one installed in load number 16), except in two loads in which is simulated the installation of two PV systems with a lower producibility in order to don't exceed the total installed power upper-limit of 100 kW prescribed by the law. The resulted total installed PV power, in this case, is of 98,9 kW.

The third scenario is the one that simulates the behaviour of the battery with the same load and generation profile of the second scenario.

3.3 Results

The values exported from the simulations executed in DigSILENT are the active and reactive power exchanged across the transformers and the active power, current and voltage profile of the battery. These information are better analysed and elaborated in the following sections, but first some general considerations on the behaviour of the grid can be deduced.

An important result is that all the simulations show that the grid doesn't suffer any problems about congestion and overvoltage caused by the high amount of PV electricity injection, both in the case in which the battery is installed and not. This means that there are not technical barriers from the electrical point of view in achieving an high decarbonisation of the grid thanks to RES generation. The presence of the battery however is able to provide further advantages to the grid thanks to the realization of power system functions like Peaks Shavings and Loads Leveling.

Figures 3.13 and 3.14, referred to the case without and with the industry respectively, show the daily profiles of the whole grid, both in winter and in summer, comparing what happens in the three different scenarios. In the case without the industry, the second scenario presents a load profile similar to the one of the first scenario during the hours of absent and low renewable production and a deep valley during the period of the day in which PV generation is high and back-feeding occur. The presence of the battery is able to make null the load during wide segments of the day and avoid peak demand. Also the amplitude, in terms of number of hours, of the valley is reduced, especially in the winter case. In the case in which the load profile of the industry is included into the grid, only the peak demand that occurs in the afternoon is avoided, and replaced with a negative peak in the second scenario and with a null contribution by the external grid in the third. The peak demand that occurs in the morning and in the evening need to be covered by the external grid both in the second and third scenarios.

3.3.1 Transformers

The installation of PV power systems represents a further stress for the grid and for transformers operations, with a different weight depending on the different cases. The installation of the battery is able to mitigate this stress in different measure. Below it is shown more in detail the load condition occurred at transformers for the grid configurations simulated.

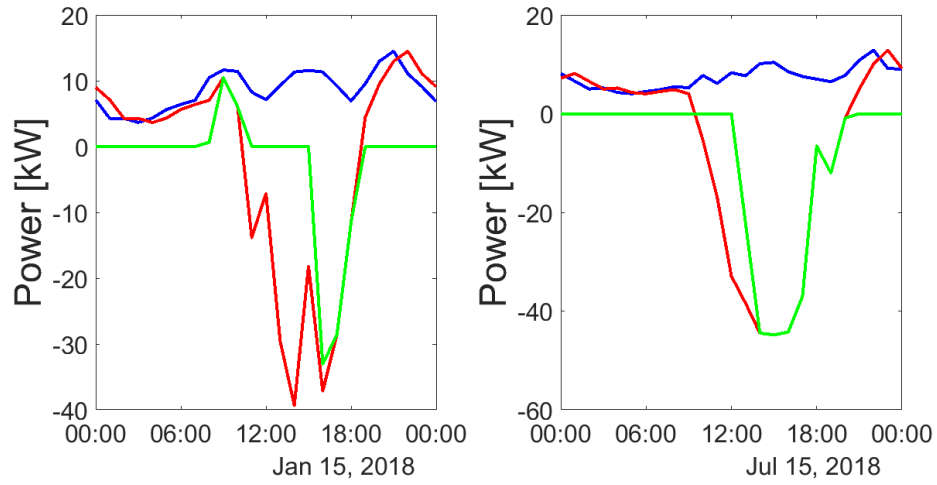


Figure 3.13: Comparison of the daily profiles of the net grid consumption in the three scenarios. Grid configuration without the factory in a winter (left) and summer (right) day.

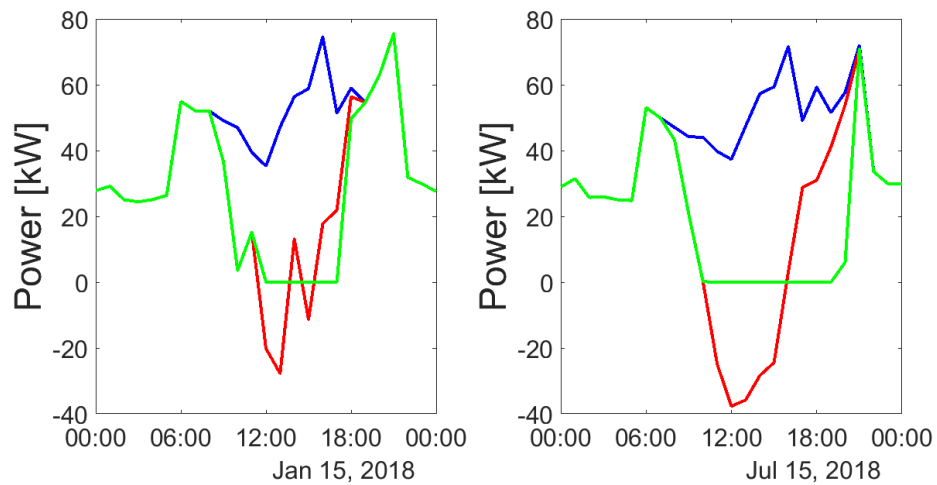
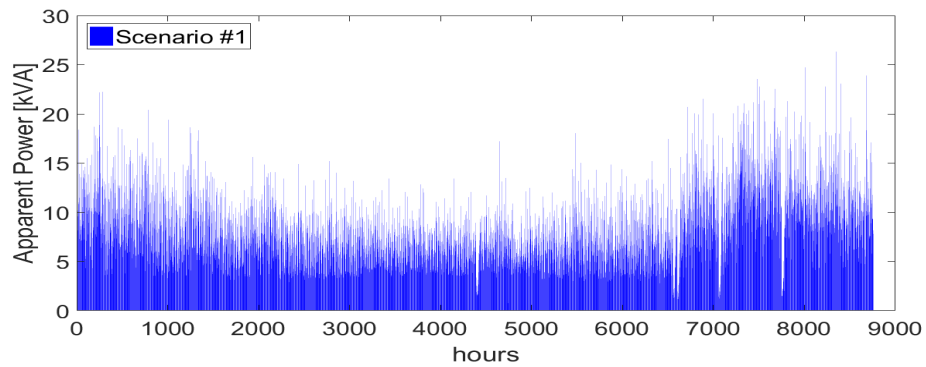


Figure 3.14: Comparison of the daily profiles of the net grid consumption in the three scenarios. Grid configuration with the factory in a winter (left) and summer (right) day.

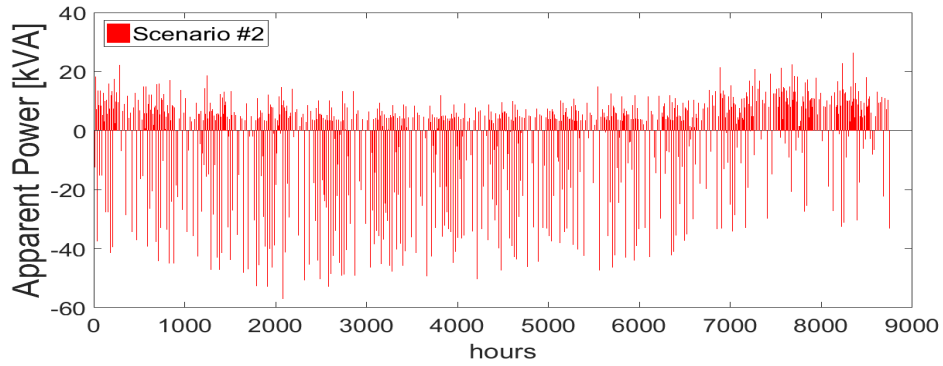
Configuration without the factory

When there is not PV integration within the grid, figure 3.15 (a), the power flow across the transformer follows only one direction, aimed to feed the grid by the external one. The integration of the PV systems generates a decrease of power demand from the external grid but introduces also the need of allow power flows across the transformers in the reverse direction (represented in 3.15 with the negative bars). The resulting power flow, due to the excess in PV generation, represents a significant load for the transformers operation: the maximum power in back-feeding is equal to 60 kW, against the maximum power demand that is equal to 28 kW (figure 3.15 (b)). The integration of the battery, as shown in figure 3.15 (c), makes null the power flow across the transformers from the external grid for the majority of

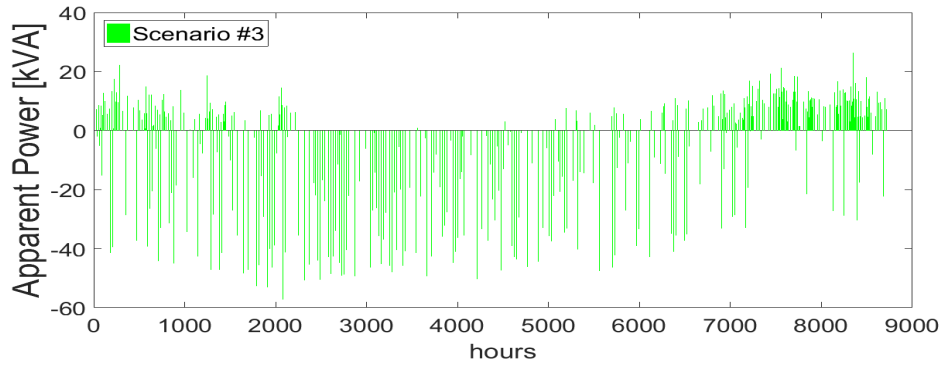
the year. Even if the value of the maximum power across the transformers doesn't decrease, the load at transformers results lower during all the rest of the year, becoming null for a considerable number of hours. Considering the scenario with the highest battery capacity (112 kWh), is possible to realize 5562 hours of grid operation in islandmode (equal to 63,5% of the year). This value can increase up to 83.3% if in this calculation is included also the number of hours in which there is an excessive PV generation, that could be curtailed if faults on the transmission network impede back-feeding. This behaviour is shown in figure 3.16, in which are represented the duration curves, obtained as the sum of the apparent power measured at the two transformers, for the three different scenarios.



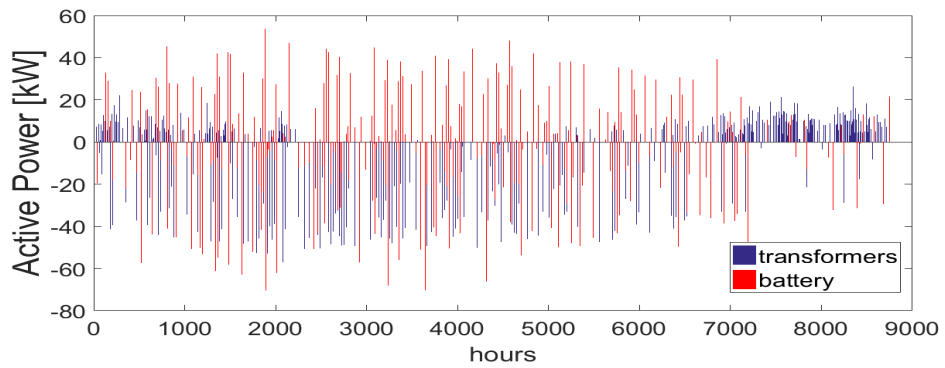
(a)



(b)



(c)

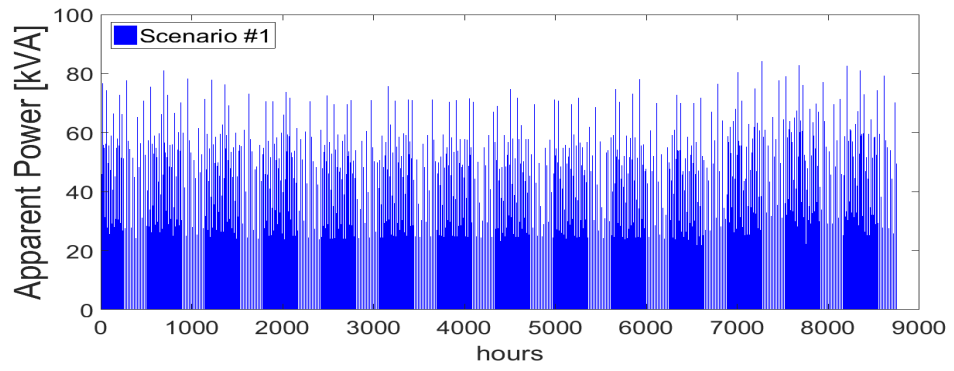


(d)

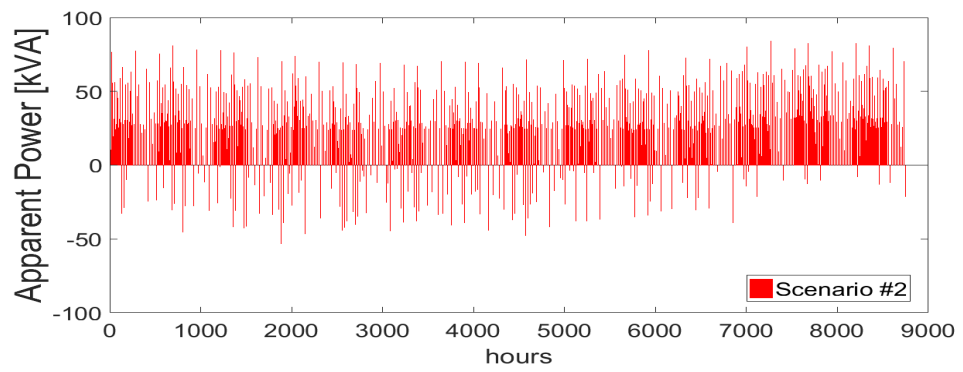
Figure 3.15: Total apparent Power across the transformers in each scenario (a - c) and comparison between the active power across the transformers and across the battery (d). Grid configuration without the factory.

Configuration with the factory

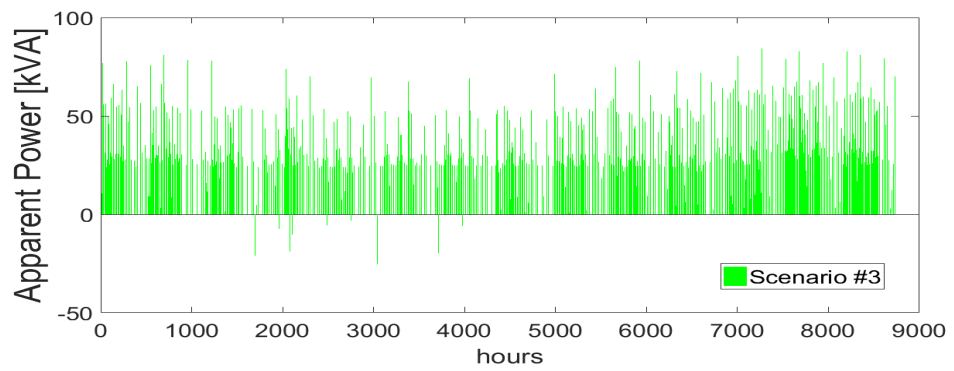
In this case, the battery and PV systems integration has a different effect on the total transformers load. The power flow due to the demand results always prevalent with respect to back-feeding one (fig. 3.17 (b)), that becomes almost null when there is the battery (fig. 3.17 (c)).



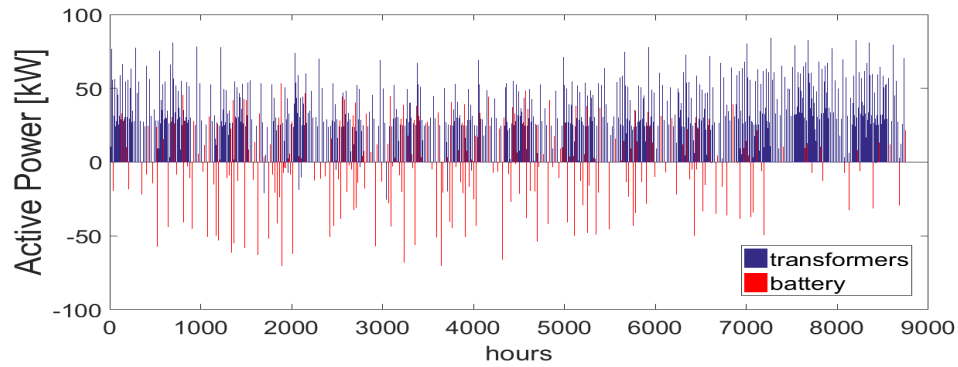
(a)



(b)



(c)



(d)

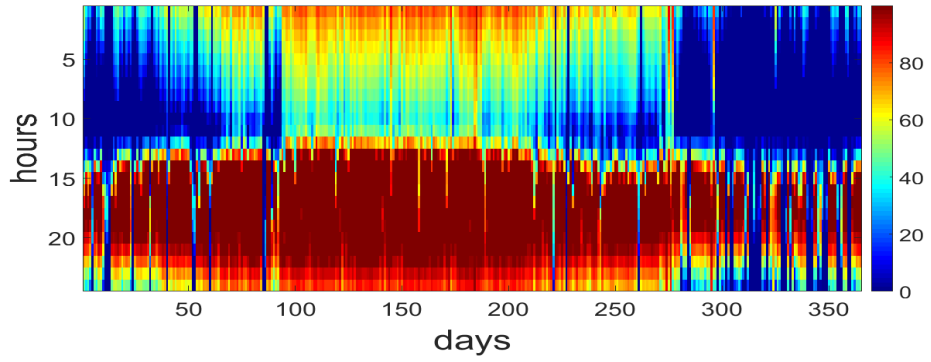
Figure 3.17: Total apparent Power across the transformers in each scenario (a - c) and comparison between the active power across the transformers and across the battery (d). Grid configuration with the factory.

Finally, the duration curves of figure 3.18 show that also in this case the presence of the battery doesn't decrease the maximum transformers load but decreases the transformers load profile in the other cases, generating a null load for the 28% of the year.

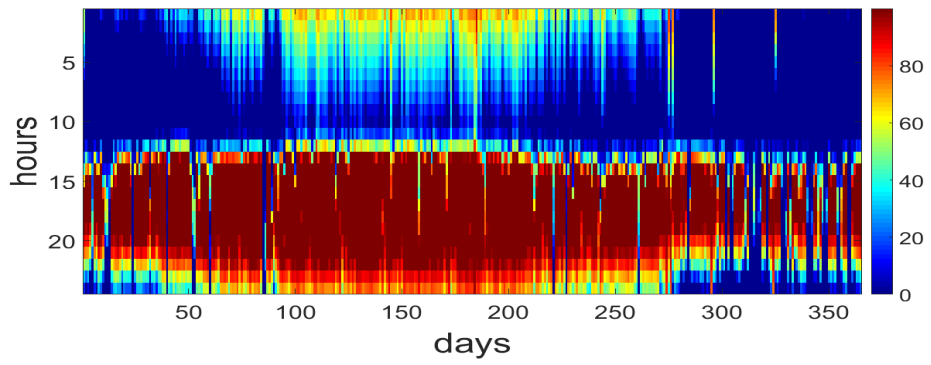
3.3.2 Battery

Configuration without the factory

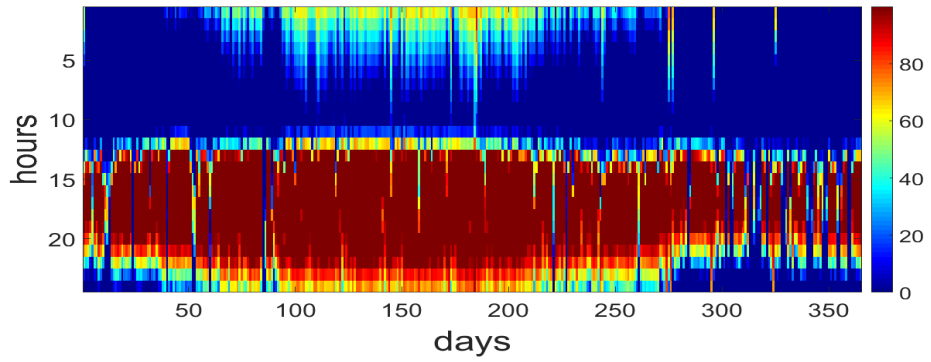
As previously told, the battery has been sized in order to cover 6 hours of grid consumption in 100%, 95%, 90% and 85% of cases. The simulations of the grid behaviour have been conducted with respect of all this 4 cases and the resulted battery operating conditions are the following. The maximum powers in charge and discharge mode occur when the battery is sized to cover 6 hours of grid consumption in 100% of cases and are 49,3 kW and 44,3 kW respectively. The percentage of hours per year during which the battery works, both in charge and discharge mode, is in the range of 84% and 60%, corresponding to a coverage of 100% and 85% of cases respectively. In all the cases the battery presents an higher state of charge during the afternoon and the evening and a lower one during the morning and the night. The range of hours per day in which the battery is fully charged increases during summer period and became shorter for decreasing value of battery capacity. In the opposite way, decreasing the battery capacity, the battery presents a fully discharged state also during summer mornings since has been fully discharged during the previous evening. Figure 3.19 shows the hourly yearly maps of the SOC of the battery, i.e. the values of the SOC obtained from the simulations and ordered for each hour and for each day of the year.



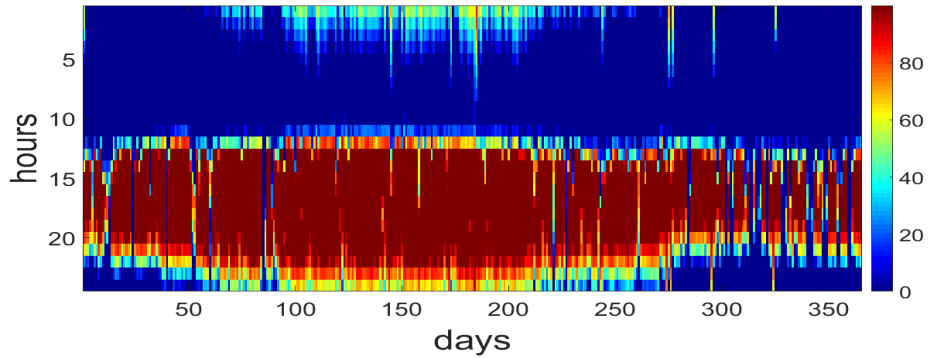
(a) Coverage in 100% of cases



(b) Coverage in 95% of cases



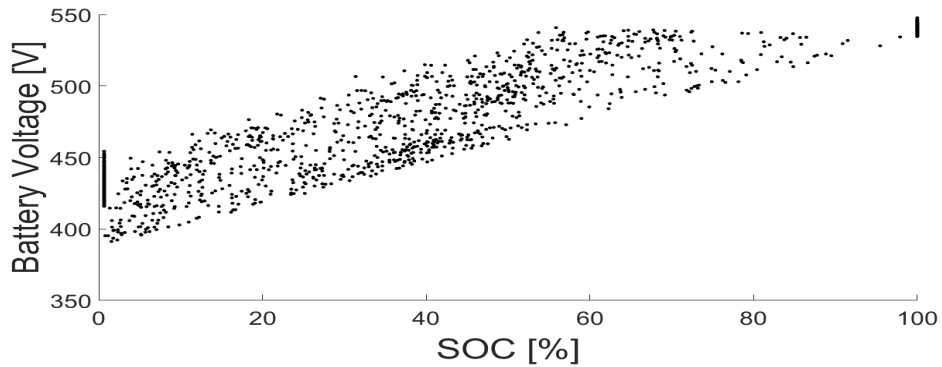
(c) Coverage in 90% of cases



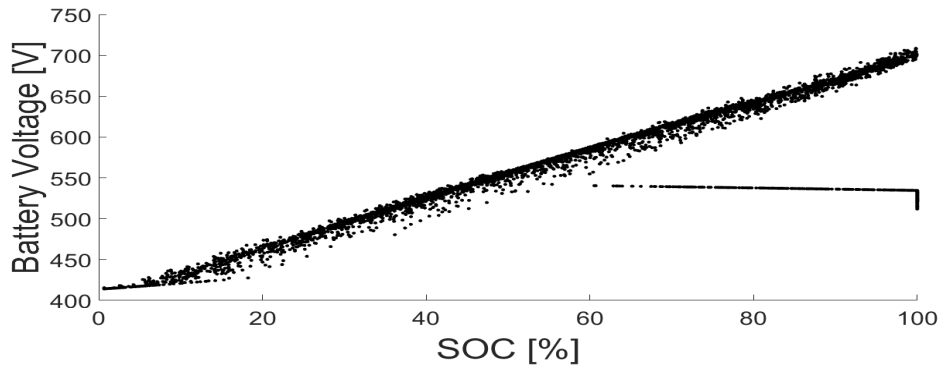
(d) Coverage in 85% of cases

Figure 3.19: Evolution of the SOC during each day of the year. Grid configuration without the factory.

Considering the voltage and the current at the ends of the battery in the case with the higher battery capacity, during its working mode the maximum voltage in charge and discharge are respectively 548 V and 709 V while the current presents higher value in charge mode than in discharge, with a maximum around 90 A in charge mode (over the battery limit) and 80 A in discharge mode. As explain in the previous section, in a battery the voltage is a function of the SOC. Even if the simulations conducted cannot be considered like the conventional tests aimed to extrapolate the discharge and charge characteristics of the battery, with the available information has been possible to build the curves of figure 3.20. While the test for the characteristics curve are executed with constant value of current, in this case the voltage value extrapolated are the ones associated to current values equals to 10%, 20% and 40% of the capacity $\pm 2,5$ A. Both in charge and discharge mode the voltage as function of the SOC has a linear behaviour.



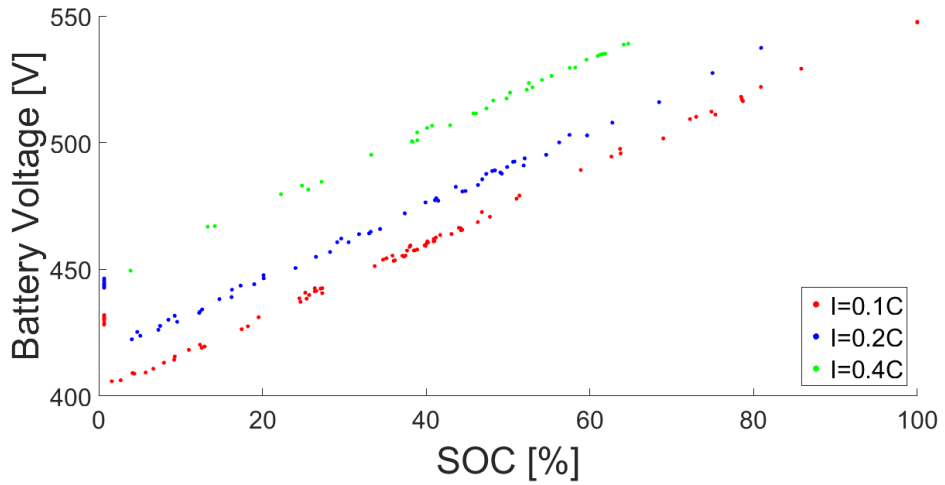
(a) Charge



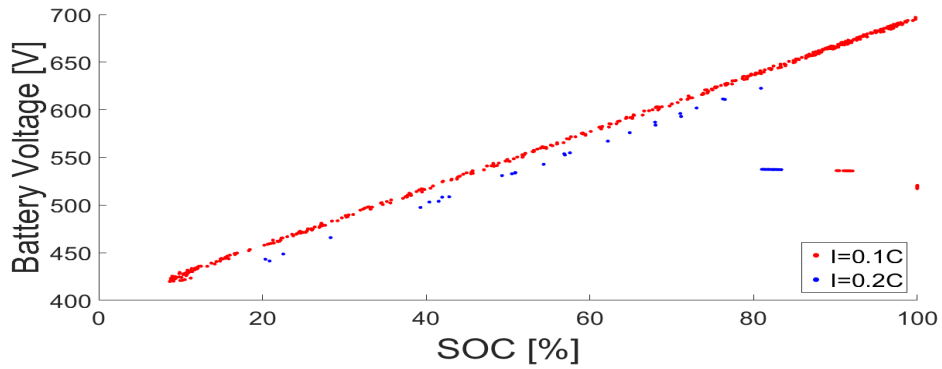
(b) Discharge

Figure 3.20: Battery voltage as function of the SOC in charge (a) and discharge (b) mode, referred to the case with a battery capacity of 112 kWh. Grid configuration without the factory.

Figure 3.21 shows how the voltage behaves during the charge and discharge phases as function of the SOC, without considering the value of the current injected or withdrawn associated to each operating condition.



(a) Charge



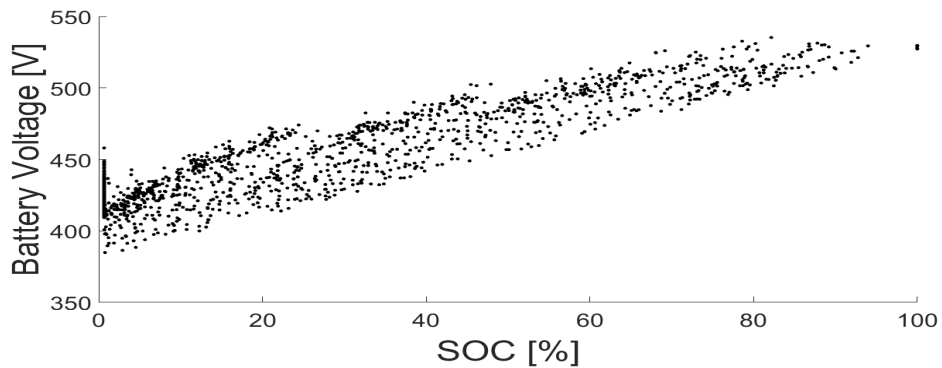
(b) Discharge

Figure 3.21: Battery voltage as function of the SOC in charge (a) and discharge (b) mode for different values of current, referred to the case with a battery capacity of 112 kWh. Grid configuration without the factory.

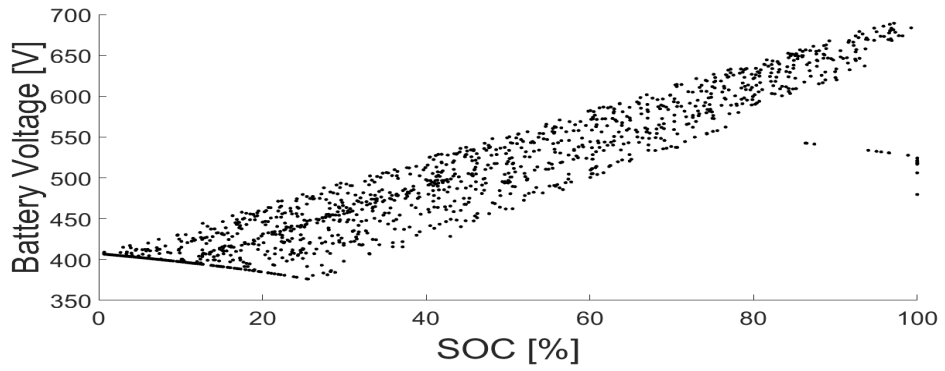
Configuration with the factory

The colormaps of figure 3.22 reveal as the battery works in a small daily range of hours, undergoing during each day a charge and discharge cycle that starts and ends with a complete discharge condition. The fraction of hours during which the battery works, both on charge and discharge mode, is around 30% for the condition with the lowest battery's capacity and increases only up to 33% in the case with the highest one. This highlights how this behaviour is not due to a not sufficient battery size, but to the fact that in this case most of the electricity is produced and consumed at the same time and that the high grid load causes a rapid battery discharge.

The graphs of figures 3.23 and 3.24 have been obtained with the same method previously explained for the scenario without the factory. Also in this case the battery voltage has a linear behaviour in function of the SOC, included in defined working regions, with higher value for higher value of current in charge mode and a opposite trend in discharge mode.

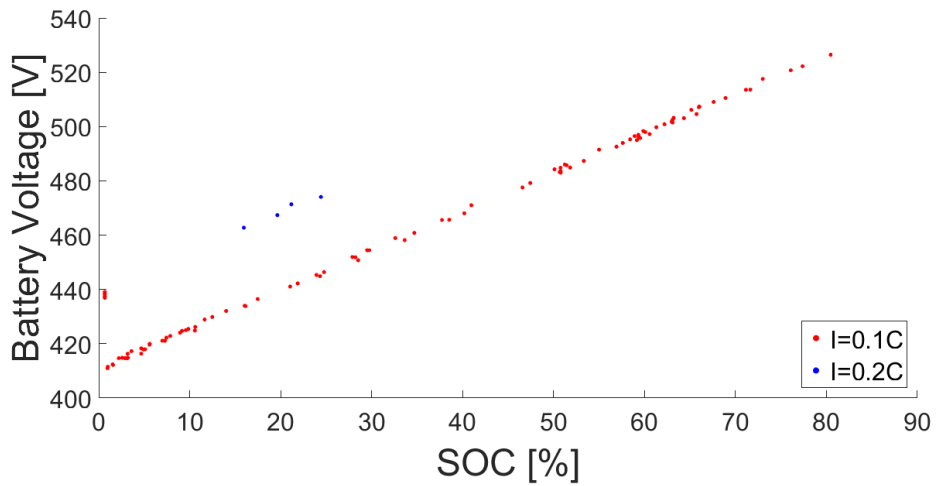


(a) Charge

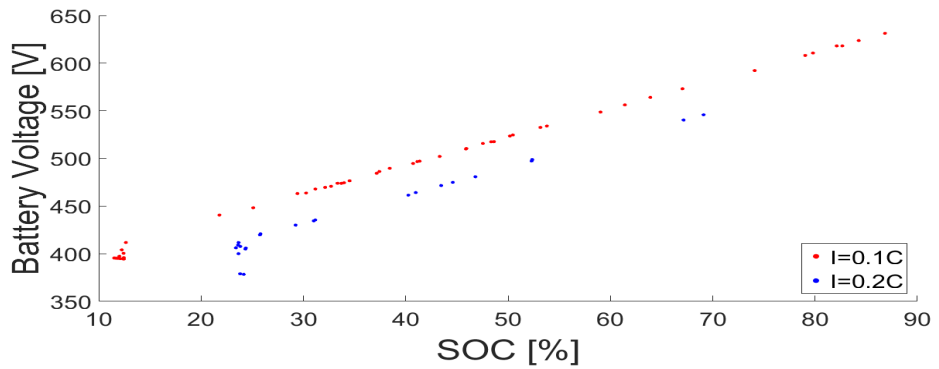


(b) Discharge

Figure 3.23: Battery voltage as function of the SOC in charge (a) and discharge (b) mode, referred to the case with a battery capacity of 177 kWh. Grid configuration with the factory.



(a) Charge



(b) Discharge

Figure 3.24: Battery voltage as function of the SOC in charge (a) and discharge (b) mode for different values of current, referred to the case with a battery capacity of 177 kWh. Grid configuration with the factory.

3.3.3 Economic feasibility

In the following table are summarized the yearly bills and yearly savings generated in each scenario.

	Factory not included						Factory included			
	S1	S2	100%		S3		S1	S2	S3	
			95%	90%	85%			0%	20%	
Yearly bill (€)	8.300	1.770	860	900	941	997	8.300	473	15	23
Savings (€)		6.530	7.440	7.400	7.360	7.303		7.827	8.285	8.277

Table 3.7: Yearly bills and savings evaluated for each scenario.

It's possible to observe how the economic savings realized with the presence of battery are not much higher than the one realized in the scenario with high PV penetration thanks to the self-consumption and to the sale of electricity surplus.

The investment cost is given by the sum of the capital cost of PV systems and of the battery. For the PV systems a cost of 1500 €/KW is assumed while the cost of the battery has been calculated considering a price of 700€/kWh.

	Factory not included	Factory included
Tot. Investment (€) (= PV Investment)	101.526	147.954
Incomes (€)	6.530	7.827
PBT (year)	16	18

Table 3.8: Investment costs and PBT of the second scenario

	Factory not included				Factory included	
	100%	95%	90%	85%	0%	20%
Battery Investment (€)	77.000	52.500	42.000	35.000	126.000	80.500
Total Investment (€)	178.526	154.026	143.526	136.526	273.954	228.454
Incomes (€)	7.440	7.400	7.360	7.303	8.285	8.277
PBT (years)	32	26	23	22	55	37

Table 3.9: Investment costs and PBT of the third scenario.

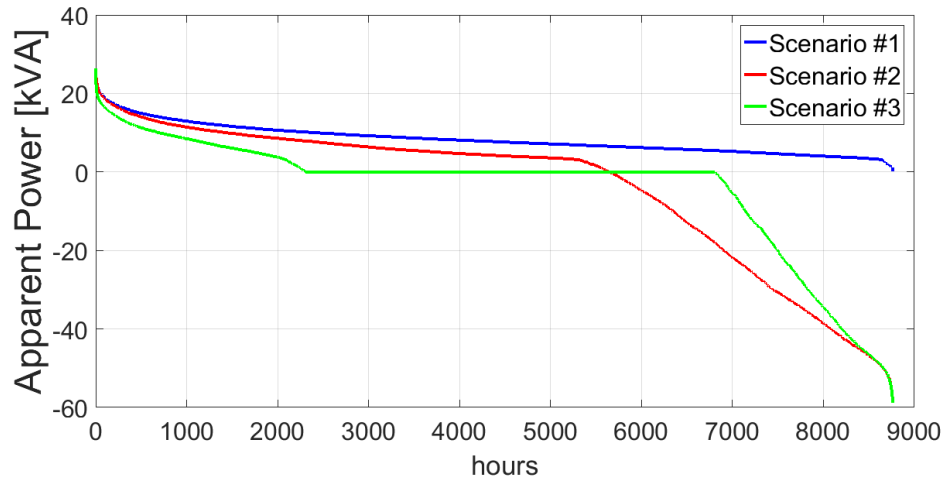


Figure 3.16: Comparison of the transformers duration curves in the three scenarios. Configuration of the grid without the factory.

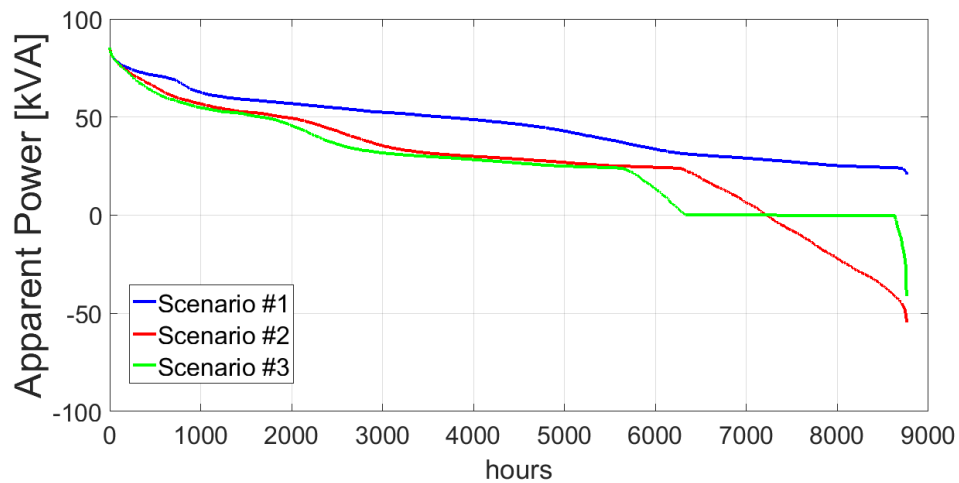
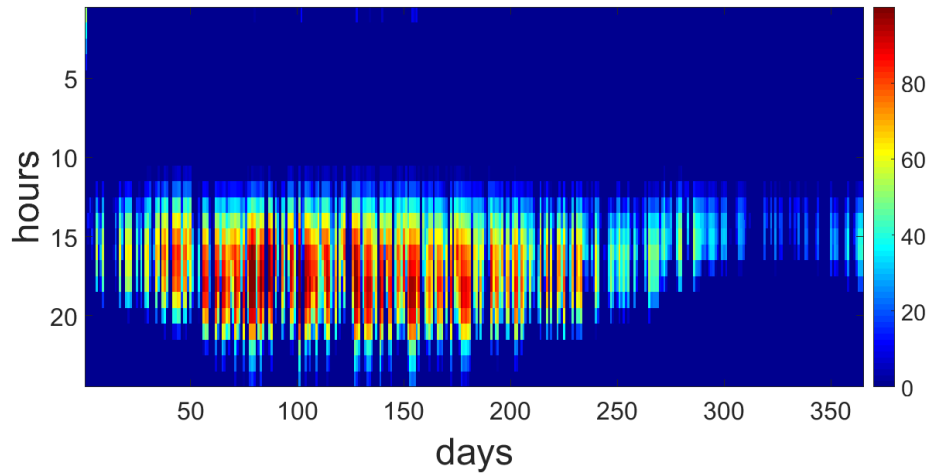
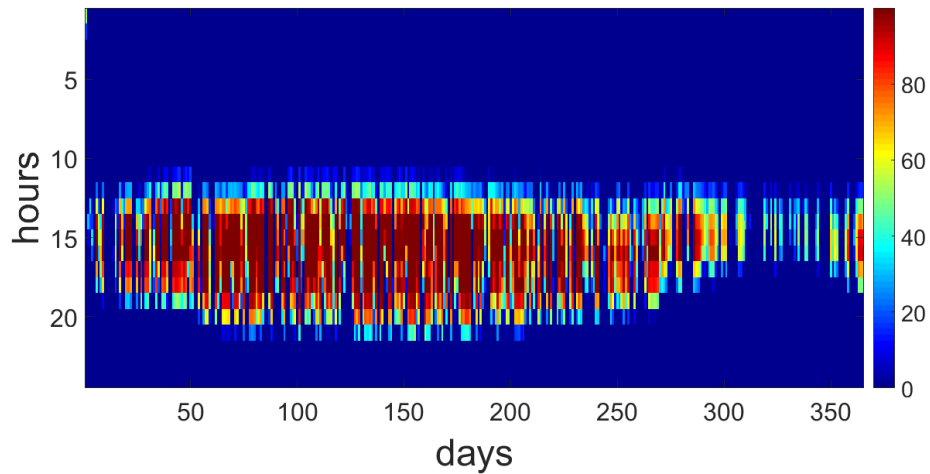


Figure 3.18: Comparison of the transformers duration curves in the three scenarios. Configuration of the grid with the factory.

From a financial point of view, a low risk scheme is adopted with a shearing of equity and debt of 50% and a cost of equity and debt equal to 3% and 5% respectively. The resulting WACC is 3,38% (eq. 2.33) while the tax rate is 25%. The Discounted Cash Flow analysis conducted brings to the calculation of the PBT. The results are summarized in table 3.9 and prove how the economical assessment of the battery integration is not positive in any scenario. In the grid configuration with the industry, the PBT of the scenarios with the battery reaches values that are not compatible with an investment in energy field of this scale and with the life time of these technologies. In the configuration with only residential users, the PBT values are significantly lower, with the best case associated to the scenario with a battery capacity of 50 kWh (S3 85%) and a PBT of 22 years. Nevertheless, also this case, considering the degradation phenomena occurring in the battery after 12 years, is not



(a) Battery capacity 177 kWh



(b) Battery capacity 114 kWh

Figure 3.22: Evolution of the SOC during each day of the year. Grid configuration with the factory.

economically convenient. What can be economically advantageous, both in the configuration with and without the factory, is the installation of PV panels, that have a PBT of 18 and 16 years respectively.

3.3.4 Environmental impact

Thanks to high PV penetration is possible to make the CO₂ footprint of the microgrid decrease of the 41% and 33% in the case without and with the factory, respectively. Besides, in the case of the grid configuration with only residential loads, an high amount of electricity is injected into the external grid. Neglecting the losses due to electricity transport and the possibility of the curtailment of the electricity excess, it's possible to avoid the production of relevant amounts of CO₂.

Considering the objective of increasing the sustainability of the microgrid, the integration

of the battery brings a relevant contribution in the grid configuration without the factory. The percentage of the decrease of the Carbon footprint grows up to 81% in the scenario with the highest battery capacity.

When the factory is included the weight of the presence of the battery is not significant as well. The percentage decrease of the CO₂ emissions is limited to 40%.

Factory not included				
Scenario	External supply (MWh)	Back-feeding (MWh)	CO ₂ footprint (ton/y)	CO ₂ footprint with PV (ton/y)
S1	73	0	21	
S2	43	-78	12,3 (-41%)	15,4 (-26%)
S3 100%	14	-49	3,9 (-81%)	7 (-66%)
S3 95%	19	-54	5,4 (-74%)	8,5 (-59%)
S3 90%	22	-58	6,4 (-69%)	9,5 (-54%)
S3 85%	26	-62	7,5 (-64%)	1,6 (-49%)

Table 3.10: Carbon footprint of the grid. Configuration without the factory.

Factory included				
Scenario	External supply (MWh)	Back-feeding (MWh)	CO ₂ footprint (ton/y)	CO ₂ footprint with PV (ton/y)
S1	397	0	113	
S2	266	-34	75,8 (-33%)	80,5 (-29%)
S3 0%	237	-4,6	66,7 (-40%)	71,3 (-37%)
S3 20%	241	-8,5	68,6 (-39%)	73,2 (-35%)

Table 3.11: Carbon footprint of the grid. Configuration with the factory.

The last columns of the previous tables show the yearly CO₂ emissions of the grid considering the PV system contributions. With an yearly energy production equal to 108 MWh and 161 MWh in the configuration without and with the factory respectively, the GHG emissions correspond to 3,1 tonCO_{2-eq}/yrs in the first case and to 4,7 tonCO_{2-eq}/yrs in the second.

The Carbon footprints of the battery production, for each value of battery capacities considered in the simulations, are listed in table 3.12. The CO₂ payback time, i.e. the time required to cover the amount of CO₂ generated because of the production of the battery thanks the CO₂ savings due to the new Carbon footprint of the whole grid, is between 2,1-1,7 years for the grid configuration without the factory and 3,1 and 2,5 years for the grid configurations with the factory. In this case the CO₂ emissions savings generated are evaluated with respect to the second scenarios, in order to isolate the battery contribution.

	Factory not included				Factory included	
	100%	95%	90%	85%	0%	20%
CO ₂ footprint Battery(ton)	18	12,2	10	8	28,5	18,3
CO ₂ payback time (years)	2,1	1,8	1,7	1,7	3,1	2,5

Table 3.12: Carbon footprint of the battery.

Chapter 4

Project Summary

In this chapter are presented the activities conducted during the elaboration of this project and an estimation of the economical cost and environmental impact associated.

4.1 Project Planning

The project has been carried out in seven months, between March and September. The first and main part of the work, i.e. the elaboration of the methodology and the simulations, has been conducted in Barcelona, in the CITCEA-UPC office, between March and July. Most of the writing has been done in the month of September, in Italy. The Gantt chart of figure 4.1 shows the temporal distribution of all the phases of the project.

4.2 Budget Estimation

This budget estimation, as the following environmental impact evaluation, is referred to the realization of this project and not to its execution, The only contribution is due to the licence of the software DigSILENT, provided by the CITCEA Department, which cost is equal to 10.000 €. The softwares used in the post processing phase are Matlab and Excel, which licences are included in the package of licences for students provided by Politecnico di Torino. Also the access to scientific periodicals has been guaranteed by Politecnico di Torino.

4.3 Environmental Impact

The environmental impact linked to the realization of this project is due to the electrical consumption caused by use of computer. Considering an average of 30-week hours of work, the total amount of hours is 720. Among them, 60% has been conducted with the CITCEA computer that consumes around 200 W, while the rest with a personal laptop that has a consumption of 90 W. The total energy consumption is of 112,32 kWh, which is associated a Carbon footprint of 32 kg CO_{2-eq}.

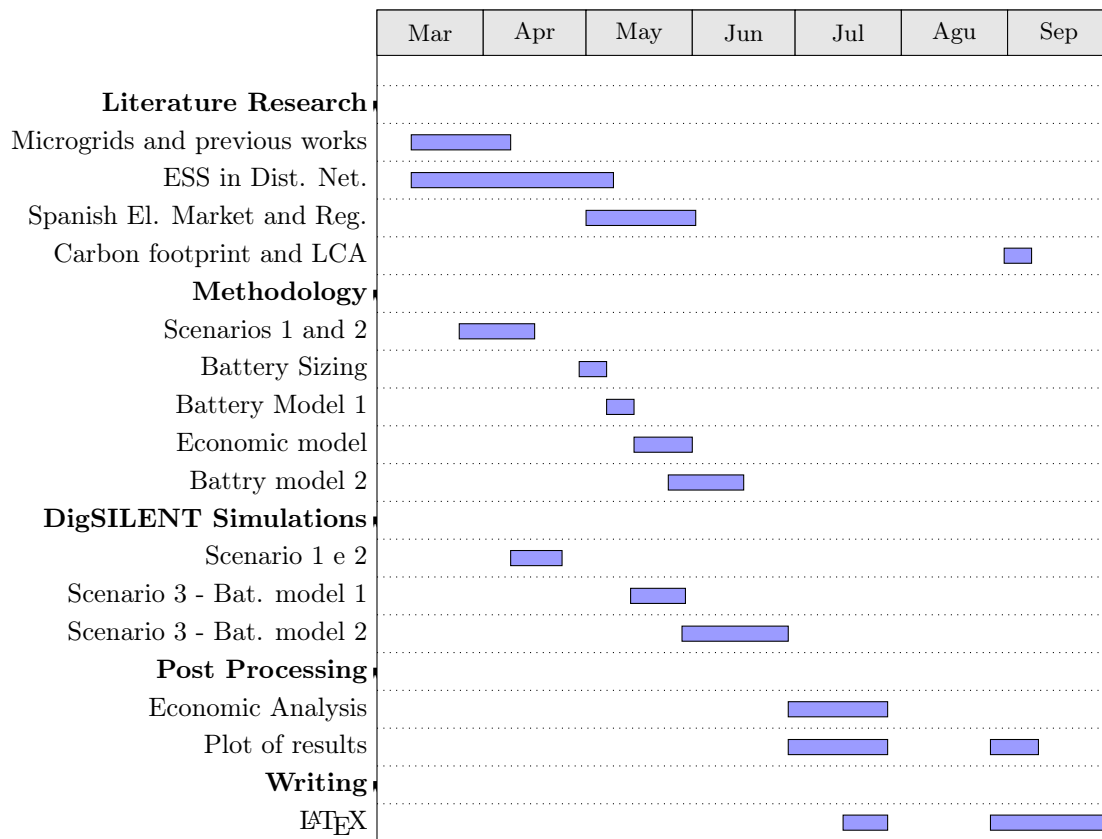


Figure 4.1: Gantt diagram of the project planning.

Chapter 5

Conclusions

In this study has been elaborated a methodology for the design and the simulation of a rural microgrid with high PV penetration and a battery storage system. This methodology has been thought for both a grid composed only by residential users and a grid that includes an industrial load. The regulatory framework within which the design choices have been taken is the one of the jointly acting self-consumption, recently regulated by the Spanish government.

The aim of the project is to increase the self-sufficiency of the grid in a sustainable way, meeting the need of rural grid of more reliability and independence from the transmission system.

The model elaborated has been applied to a study case, represented by a rural grid in Santa Maria de Corcò, in Girona.

The result obtained is that in the configuration with only residential users the installation of PV power systems generates an electricity surplus that would justify the presence of a storage system, able to provide UPS, peak shaving and loads leveling. In the scenario with the installation of a battery with a capacity of 112 kWh the microgrid can operate in islandmode between the 63,5% and the 83,3% of the time during the year. The lower value is evaluated on the bases of the number of hours per year in which the grid doesn't exchange power with the external grid. The higher one takes into account the possibility of disconnect the microgrid from the external one also during the hours in which there is an excess in PV generation. In this way, the requirement of increase the independence and the reliability in case of faults in the external systems is effectively satisfied. From the economical point of view, the project has not a positive assessment because the PBT obtained for all the battery capacity scenarios simulated reaches values not compatible with the life time of the technologies. The environmental impact evaluation presents good results: the carbon footprint of the microgrid decreases of a percentage between 64% and 81%. These values became 49% and 66% if the virtual yearly emissions due to the PV systems life cycle are taken into account. The LCA study referred to the battery allows to estimate a CO₂ payback time of the battery between 1,7 and 2,1 years.

Thus, the drivers for the realization of the project are improving the quality of the electricity service, increasing the guarantee of a continuous supply, and making the grid Carbon footprint dramatically decrease. On the other side, an economical barrier exists: the new possibilities provided by the Self-consumption Royal Decree are not sufficient for supporting batteries integration. The current batteries price is still high and can't be born by prosumers citizens. Other contributions are needed as, for example, government subsidies or the distribution utility participation to the investment. In fact, since the presence of the battery is able to decrease the load on transformers, distribution utility could benefit from

the installation of a battery instead of making other investment on the transformers and on the network.

With the constrains taken into account in this work, the installation of only PV power systems results advantageous: it does not generate problems of congestion or overload of cables and transformers, has an acceptable PBT and reduces the Carbon footprint of the grid of 41% (28% considering the PV systems contribute). Moreover 78 MWh/year of clean energy are inject into the external grid, that, if produced with conventional power plants, would generate 22 ton of CO₂.

Similar consideration can be done for the grid configuration that includes the factory. Also in this case, the installation of PV power systems has a positive impact and results economically advantageous. It reduces the grid load during the central hours of the day, decreasing the transformers load. The emissions of CO₂ decrease of 33% (29% with PV system contribute) and 34 MWh/year are injected into the external grid.

The installation of a battery in this case is absolutely not practical from an economical point of view and concerning environmental and reliability issues doesn't generate effects significant as in the previous case. The percentage of hour during the year in which the grid operates in islandmode is of 28% and the add of a battery increases the CO₂ emission reduction just up to 40%. This is because most of the electricity surplus produced by the jointly acting self-consumers group is consumed within the grid.

In order to increase the indipendence of the microgrid is necessary to design a solution suitable for covering the industry load, that involves the industry itself and the distributor utility.

Bibliography

- [1] 4th benchmarking report on quality of electricity supply, page 22. Technical report, Council of European Energy Regulators, 2008.
- [2] Ceer benchmarking report 5.2 on the continuity of electricity supply, page 15 and page 39. Technical report, Council of European Energy Regulators.
- [3] Romain Debarre Benoit Decurt, Bruno Lajoie and Olivier Soupa. Hydrogen-based energy conversion - more than storage: System flexibility. Technical report, SBC Energy Institute.
- [4] Bruce Dunn, Haresh Kamath, and Jean-Marie Tarascon. Electrical energy storage for the grid: A battery of choices. *Science*, 334(6058):928–935, 2011.
- [5] Description of the operation of the mibel. Technical report, MIBEL Regulatory Council.
- [6] Energia y sociedad. Manual de la energia.
- [7] ESIOS: Sistema de informaci3n del operador del sistema. Self-consumption surplus energy price for the simplified compensation mechanism (pvpc).
- [8] Red Electrica de Espana. Informe del sistema el3ctrico espa1ol 2017.
- [9] P. Sinha M. de Wild-Scholten J. Zhang V. Fthenakis H. C. Kim M. Raugei M. Stucki R. Frischknecht, R. Itten. Life cycle inventories and life cycle assessment of photovoltaic systems.
- [10] FENECON. «fenecon comercial 50-serie,» fenecon gmbh, deggendorf, germany, 2018.
- [11] Center for Advanced Life Cycle Engineering CALCE. Inr 18650-20r cells.
- [12] Communication from the commission to the european parliament, the european council, the council, the european economic and social committee, the committee of the regions and the european investment bank: A clean planet for all, a european strategic long-term vision for a prosperous, modern, competitive and climate neutral economy. , European Commission, 2018.
- [13] Communication from the commission to the european parliament, the council, the european economic and social committee and the committee of the regions: Energy roadmap 2050. , European Commission, 2011.
- [14] Dan T. Ton and Merrill A. Smith. The u.s. department of energy’s microgrid initiative. *The Electricity Journal*, 25(8):84 – 94, 2012.
- [15] Toby Considine, William Cox, and Edward G Cazalet. Understanding microgrids as the essential architecture of smart energy. 12 2012.

- [16] Yael Parag and Malcolm Ainspan. Sustainable microgrids: Economic, environmental and social costs and benefits of microgrid deployment. *Energy for Sustainable Development*, 52:72 – 81, 2019.
- [17] Fact sheet - jobs in renewable energy and energy efficiency. Technical report, Environmental and Energy Studies Institute.
- [18] Integrating high levels of renewables into microgrids. Technical report, ABB.
- [19] Vinodkumar Etacheri, Rotem Marom, Ran Elazari, Gregory Salitra, and Doron Aurbach. Challenges in the development of advanced li-ion batteries: A review. *Energy Environmental Science*, 4, 01 2011.
- [20] Yonghuan Ren Borong Wu and Ning Li. *LiFePO₄ cathode material*. In: *Soylu S (ed) Electric vehicles, the benefits and barriers. InTech*, p. 199–216.
- [21] Andrew W. Thompson. Economic implications of lithium ion battery degradation for vehicle-to-grid (v2x) services. *Journal of Power Sources*, 396:691 – 709, 2018.
- [22] Directive 2009/72/ec of the european parliament and of the council of 13 july 2009 concerning common rules for the internal market in electricity and repealing directive 2003/54/ec. Technical report, THE EUROPEAN PARLIAMENT AND THE COUNCIL OF THE EUROPEAN UNION.
- [23] Giorgio Castagneto Gisse, Paul E. Dodds, and Jonathan Radcliffe. Market and regulatory barriers to electrical energy storage innovation. *Renewable and Sustainable Energy Reviews*, 82:781 – 790, 2018.
- [24] Danny Pudjianto Predrag Djapic Fei Teng Alexander Sturt Dejvise Jackravut Robert Sansom Vladimir Yufit Nigel Brandon Goran Strbac, Marko Aunedi. Strategic assessment of the role and value of energy storage systems in the uk low carbon energy future. Technical report, Imperial Collage London.
- [25] Clean energy for all europeans. Technical report, Directorate-General for Energy (European Commission), 2019.
- [26] Directive (eu) 2018/2001 of the european parliament and of the council of 11 december 2018 on the promotion of the use of energy from renewable sources. Technical report, THE EUROPEAN PARLIAMENT AND THE COUNCIL OF THE EUROPEAN UNION.
- [27] *Real Decreto 244/2019, de 5 de abril, por el que se regulan las condiciones administrativas, técnicas y económicas del autoconsumo de energía eléctrica*.
- [28] John G. Wimer and Wm Morgan Summers. Quality guideline for energy system studies: Cost estimation methodology for netl assessments of power plant performance. 4 2011.
- [29] Crporate taxes rates. Technical report, Deloitte, 2019.
- [30] Gaëtan Masson and izumi Kaizuka. Trends in photovoltaic applications survey report of the selected iea countries in 2018. Technical report, International Energy Agency (IEA), 2018.
- [31] Norasikin Ahmad Ludin, Nur Ifthitah Mustafa, Marlia M. Hanafiah, Mohd Adib Ibrahim, Mohd Asri Mat Teridi, Suhaila Sepeai, Azami Zaharim, and Kamaruzzaman Sopian. Prospects of life cycle assessment of renewable energy from solar photovoltaic technologies: A review. *Renewable and Sustainable Energy Reviews*, 96:11 – 28, 2018.

- [32] Anderik Alsema Vasilis M. Fthenakis, Hyung Chul Kim. Emissions from photovoltaic life cycles. *environmental science technology*. 42(6).
- [33] K. Wambach P. Sinha G. Heath P. Stolz, R. Frischknecht. Life cycle assessment of current photovoltaic module recycling. Technical report, International Energy Agency Power Systems Programme.
- [34] Jens F. Peters, Manuel Baumann, Benedikt Zimmermann, Jessica Braun, and Marcel Weil. The environmental impact of li-ion batteries and the role of key parameters – a review. *Renewable and Sustainable Energy Reviews*, 67:491 – 506, 2017.
- [35] Lisbeth Dahllöf Mia Romare. The life cycle energy consumption and greenhouse gas emissions from lithium-ion batteries. Technical report, IVL Swedish Environmental Research Institute.